



# Mast cell activation induced by tamoxifen citrate via MRGPRX2 plays a potential adverse role in breast cancer treatment

Jiapan Gao<sup>a,b,1</sup>, Xinyue Su<sup>a,b,1</sup>, Yuxiu Zhang<sup>a,b</sup>, Xiaoyu Ma<sup>a,b</sup>, Bingxi Ren<sup>a,b</sup>, Panpan Lei<sup>a,b</sup>, Jiming Jin<sup>c</sup>, Weina Ma<sup>a,b,\*</sup>

<sup>a</sup> School of Pharmacy, Xi'an Jiaotong University, Xi'an 710061, PR China

<sup>b</sup> State Key Laboratory of Shaanxi for Natural Medicines Research and Engineering, Xi'an 710061, PR China

<sup>c</sup> First School of Clinical Medicine, Shaanxi University of Chinese Medicine, Xi'an 712046, PR China

## ARTICLE INFO

### Keywords:

Breast cancer  
Tamoxifen citrate  
MRGPRX2  
Mast cell activation  
Proliferation  
Migration

## ABSTRACT

Breast cancer is the most common malignant tumor endangering women's life and health. Tamoxifen citrate (TAM) is the first-line drug of adjuvant endocrine therapy for estrogen receptor-positive (ER<sup>+</sup>) breast cancer patients. Some sporadic cases have described rare adverse reactions of TAM with potentially life-threatening dermatological manifestations, which were associated with skin allergy. Mas related G protein-coupled receptor X2 (MRGPRX2) on human mast cells is the key target for skin allergy. We aimed to investigate the mechanism of TAM-induced allergic reactions and their potential effects on TAM treatment for breast cancer. In our study, TAM can specifically bind with MRGPRX2, which was mainly driven by hydrophobic force. TAM formed hydrogen bonds with TRP243, TRP248, and GLU164 residues in MRGPRX2. TAM induced calcium mobilization and degranulation of mast cells via MRGPRX2. Besides, TAM induced passive cutaneous anaphylaxis and active systemic anaphylaxis in C57BL/6 mice. The release of  $\beta$ -hexosaminidase, histamine, tumor necrosis factor- $\alpha$ , monocyte chemoattractant protein 1, and interleukin-8 were increased by TAM *in vitro* and *in vivo*. Furthermore, we found that MCF-7 and T-47D breast cancer cells can recruit mast cells to adjacent cancerous tissues. Besides, mast cell activation induced by TAM via MRGPRX2 significantly promoted the proliferation and migration of MCF-7 and T-47D cells, which can be effectively reversed by mast cell membrane stabilizer clarithromycin and MRGPRX2 silencing. This study proposed an anti-allergic therapeutic strategy for breast cancer treatment with TAM, while also the potential of MRGPRX2 as an adjunctive target.

## 1. Introduction

Breast cancer is the second largest cancer worldwide, with incidence and mortality ranking first among female malignant tumors [1]. Estrogen receptor-positive (ER<sup>+</sup>) breast cancer is the most common breast cancer subtype. Tamoxifen citrate (TAM) is the first-line drug of adjuvant endocrine therapy for ER<sup>+</sup> breast cancer patients, which can significantly reduce the risk of recurrence and death of breast cancer [2]. The clinical adverse reactions of TAM were mostly mild in symptoms,

and a variety of rashes have been reported to date [3]. However, some sporadic cases have described rare adverse reactions of TAM, such as erythema multiforme, bullous pemphigus, vasculitis, angioedema, baboon syndrome, etc. [4–7], most of which were associated with skin allergy. Given the widespread use of TAM in breast cancer patients, it was necessary to recognize the rare, but potentially life-threatening dermatological manifestations of TAM use.

Mast cells are important effector cells that mediate inflammation and allergic reactions [8]. The drug-induced allergic reactions are

**Abbreviations:** ASA, active systemic anaphylaxis; AZT, azidothymidine; C48/80, compound C48/80; CCK-8, cell counting kit-8; CIB, calcium imaging buffer; CIP, ciprofloxacin hydrochloride; CLA, clarithromycin; CMC, cell membrane chromatography; CMs, conditioned mediums; ER<sup>+</sup>, estrogen receptor-positive; IL-8, interleukin-8; LAD2 cells, human laboratory of allergic disease 2 mast cells; MCP-1, monocyte chemoattractant protein 1; MRGPRX2, mas related G protein-coupled receptor X2; MRGPRX2-HEK293 cells, MRGPRX2-expressing HEK293 cells; MTT, 3-(4,5-dimethyl-2-thiazolyl)-2,5-diphenyl-2-H-tetrazolium bromide; PCA, passive cutaneous anaphylaxis; TAM, tamoxifen citrate; TNF- $\alpha$ , tumor necrosis factor- $\alpha$ .

\* Corresponding author at: School of Pharmacy, Xi'an Jiaotong University, Yanta Westroad, Xi'an 710061, PR China.

E-mail address: [maweina2015@xjtu.edu.cn](mailto:maweina2015@xjtu.edu.cn) (W. Ma).

<sup>1</sup> These authors contributed equally to this work.

<https://doi.org/10.1016/j.bcp.2025.116760>

Received 5 August 2024; Received in revised form 8 October 2024; Accepted 14 January 2025

Available online 18 January 2025

0006-2952/© 2025 Elsevier Inc. All rights are reserved, including those for text and data mining, AI training, and similar technologies.

conventionally attributed to the mechanism mediated by immunoglobulin E (IgE) [9]. However, it was reported that preventive and therapeutically TAM treatment effectively reduced allergen-specific Ig levels (IgE, IgG1 and IgG2a), and improved allergen-induced dermatitis by interfering with the allergic immune response [10]. This indicated that the allergic reactions induced by TAM were independent of IgE. Mas related G protein-coupled receptor X2 (MRGPRX2) is a biomarker of connective tissue mast cells and is abundant in skin [11]. In 2015, McNeil et al. [12] firstly reported that MRGPRX2 on human mast cells (mouse homologous Mrgprb2) can be recognized by endogenous peptides and small molecule compounds, triggering mast cell degranulation and systemic allergic reactions. Many drugs have been reported to trigger pseudo-allergic reactions via MRGPRX2, including muscle relaxants, peptide drugs, tetrahydroisoquinolines, quinolone antibiotics, analgesics, etc [13–19]. MRGPRX2-mediated mast cell activation was also involved in some skin allergic diseases (such as urticarial, atopic dermatitis, allergic contact dermatitis, red person syndrome and rosacea) [20–23], as well as the course of pain, itching, skin flushing and increased vascular permeability, which were typical symptoms of pseudo-allergic reactions [24]. As above, MRGPRX2 was speculated to be the target receptor for skin allergies in clinical TAM treatment for breast cancer.

At present, the effect of mast cells on tumor progression is still controversial [25]. Activated mast cells can regulate cancer immunity by secreting inflammatory mediators, which led to contradictory effects on tumor deterioration or therapy [26]. In addition to the direct effect of mast cell activation on tumor progression, mast cells can also be recruited by other cells, and indirectly participate in cancer development by regulating immune cells to reshape the tumor microenvironment [26]. It was found that the presence of stromal mast cells in breast cancer correlated to low grade tumours and ER<sup>+</sup> status [27]. The density of mast cells in tumor tissue was positively correlated with the poor prognosis of canine breast cancer, which could be used to evaluate the invasiveness of breast cancer [28]. The killer cell immunoglobulin-like receptor was firstly detected in human mast cells, which can promote the invasion and metastasis of breast cancer expressing human leukocyte antigen-G [29]. Moreover, mast cells can increase the expression of ER and its downstream progesterone-receptor, B-cell lymphoma 2, which promoted the growth of primary breast cancer in mice, and made more breast cancer cells develop into luminal subtype [30]. As above, high tumor mast cell density was usually associated with poor prognosis or unfavorable clinical outcomes and aggressive features of breast cancer, which indicated that mast cells were most likely to play adverse roles in breast cancer.

In summary, TAM is expected to trigger mast cell activation via MRGPRX2, which mediates the occurrence of drug allergic reactions; Meanwhile, the large number of mast cells in tumor tissues could negatively affect the onset and progression of breast cancer. Consequently, the aim of this study was to determine if TAM-induced allergic reactions correlated to MRGPRX2, and further examine the potential roles of MRGPRX2-mediated mast cell activation on the course of TAM treatment for breast cancer. Our study will deepen the understanding of the mechanisms of allergic reactions induced by TAM treatment for breast cancer, and is beneficial to provide an optimized therapeutic strategy for breast cancer.

## 2. Materials and methods

### 2.1. Chemicals and reagents

Tamoxifen citrate (TAM, purity > 98%) was purchased from Dalian Meilun Biotechnology Co., Ltd (Dalian, Liaoning, China). Evans blue, compound 48/80 (C48/80), *p*-nitrophenyl *N*-acetyl- $\beta$ -D-glucosamide, triton X-100, and 3-(4,5-dimethylthiazol-2-yl)-2,5-diphenyltetrazolium bromide (MTT) were purchased from Sigma-Aldrich (St. Louis, MO, USA). Cell counting kit-8 (CCK-8) were purchased from 7Sea

Pharmatech Co., Ltd (Shanghai, China). Ciprofloxacin hydrochloride (CIP, purity > 98%), azidothymidine (AZT, purity > 98%), and clarithromycin (CLA, purity > 98%) were purchased from Shanghai yuanye Bio-technology Co., Ltd (Shanghai, China). Histamine and histamine-d4 were obtained from Sigma (San Francisco, CA, USA). Fluo-3, AM ester and Pluronic F-127 were obtained from Biotium (Bay Area, CA, USA). Smart pools of double-stranded siRNAs targeting MRGPRX2 and non-specific siRNAs were obtained from Shanghai GenePharma Co., Ltd (Shanghai, China). Lipofectamine<sup>TM</sup> 3000 was purchased from Invitrogen Corporation (Carlsbad, CA, USA). Tumor necrosis factor- $\alpha$  (TNF- $\alpha$ ), monocyte chemoattractant protein 1 (MCP-1) and interleukin-8 (IL-8) ELISA kits (human and mouse) were obtained from ExCell Biology, Inc. (Shanghai, China). The primers for MRGPRX2 and PrimeScrip<sup>TM</sup> RT reagent kit were purchased from Takara Biotechnology Co., Ltd. (Dalian, Liaoning, China).

### 2.2. Animals

Male C57BL/6 mice aged 6–8 weeks were used and raised in the Experimental Animal Center of Xi'an Jiaotong University (Xi'an, China), with food and water freely available. The Animal Ethics Committee of Xi'an Jiaotong University approved the animal experimental protocols performed in this study (Permit Number: XJTU 2021–1561).

### 2.3. Cell lines

HEK293 cells were constructed by Jiman Biotechnology Co., Ltd (Shanghai, China). HEK293 cells with high expression of MRGPRX2<sup>N</sup>-SNAP-tag (MRGPRX2-HEK293 cells) were constructed by Saiye Biotechnology Co., Ltd (Guangzhou, Guangdong, China). Human laboratory of allergic disease 2 mast cells (LAD2 cells) were kindly provided by A. Kirshenbaum and D. Metcalfe (NIH). Human noncancerous breast cell line (MCF-10A) and human breast cancer cell lines (MCF-7 and T-47D) were from the National Experimental Cell Resource Sharing Platform (Beijing, China).

MRGPRX2-HEK293 cells were cultured in DMEM medium containing 10% fetal bovine serum (Thermo Fisher Scientific, MA, USA), 100 U/mL penicillin–streptomycin (1:1) (MedChemExpress, NJ, USA), and 0.5  $\mu$ g/mL puromycin (Meilun, Dalian, China). LAD2 cells were maintained in StemPro<sup>TM</sup>-34 medium supplemented with 10 mL/L StemPro<sup>TM</sup> nutrient supplement (Gibco, CA, USA), 1:100 penicillin–streptomycin, 2 mM L-glutamine and 100 ng/mL human stem cell factor (Peprotech, NJ, USA). MCF-10A cells were cultured in DMEM/F12 medium containing 5% horse serum (Thermo Fisher Scientific, MA, USA), 20 ng/mL epidermal growth factor (Peprotech, NJ, USA), 10  $\mu$ g/mL insulin (Sigma-Aldrich, MO, USA), 0.5  $\mu$ g/mL hydrocortisone (Sigma-Aldrich, MO, USA), 0.1  $\mu$ g/mL cholera toxin (Sigma-Aldrich, MO, USA), and 100 U/mL penicillin–streptomycin (1:1). HEK293, MCF-7 and T-47D cells were cultured in DMEM medium containing 10% fetal bovine serum, 100 U/mL penicillin–streptomycin (1:1). Cells were cultured in a 37°C incubator containing 5% CO<sub>2</sub>.

### 2.4. Construction of MRGPRX2-HEK293/cell membrane chromatography (CMC) model

MRGPRX2-HEK293 cells ( $5 \times 10^6$  cells) were digested with trypsin and washed 3 times with PBS. The cells were then broken with 5 mL Tris-HCl (50 mM, pH 7.4) by a JY92-IIN ultrasonic cell grinder (Ningbo Scientz, Zhejiang, China). After that, the cell suspension was centrifuged at 3000 rpm for 10 min; the supernatant was collected followed by centrifugation at 12,000 rpm for 20 min to obtain the cell membrane precipitation. Subsequently, the cell membrane precipitation was captured onto 0.05 g of BG-derivative-modified silica gel in 1 mL of PBS at 37°C, 1500 rpm for 30 min, using a ThermoMixerC thermal mixer (Eppendorf, Hamburg, Germany). Finally, the stationary phases were wet packed into the CMC columns by a RPL-ZD10 loading machine

(Dalian Ripuli, Liaoning, China), with a flow rate of 1 mL/min and a pressure below 5 MPa. All samples were dissolved in methanol to a concentration of 1 mg/mL, and then filtered with 0.45  $\mu\text{m}$  membrane filter. A Shimadzu LC-20A high performance liquid chromatograph (Kyoto, Japan) was used for chromatographic analysis, with a constant flow rate of 0.2 mL/min at 238 nm in 37°C. 5  $\mu\text{L}$  of the samples were injected into the CMC columns that pre equilibrated with water, and the affinity curves of the compounds for specific binding to MRGPRX2 were obtained based on chromatographic principles.

## 2.5. Stepwise frontal analysis

The stepwise frontal method is a technique derived from frontal analysis theory that can determine the  $K_D$  value of drug-receptor interactions through continuous injection. The CMC column (1 mm I.D.  $\times$  1 mm) was equilibrated with water (mobile phase A) for 1–2 h.  $1 \times 10^{-6}$  M TAM prepared in water was considered as mobile phase B. Breakthrough curves were formed by sequential entry of TAM from low to high concentrations of  $2 \times 10^{-7}$ ,  $4 \times 10^{-7}$ ,  $6 \times 10^{-7}$ ,  $8 \times 10^{-7}$ , and  $1 \times 10^{-6}$  M into the column. The time required for each concentration of TAM to reach the detection platform was recorded. Once the prior concentration of TAM reached platform stage in the CMC column, the next concentration of TAM began to flow in. The gradient elution procedure was as follows: 0  $\rightarrow$  60 min, 20% (B); 60.1  $\rightarrow$  90 min, 40% (B); 90.1  $\rightarrow$  120 min, 60% (B); 120.1  $\rightarrow$  150 min, 80% (B); 150.1  $\rightarrow$  180 min, 100% (B). The detection was performed at 238 nm in 37°C, with a flow rate of 0.6 mL/min. Breakthrough curves of AZT (a negative control) were obtained in the same way to determine the dead volume of the MRGPRX2-HEK293/CMC system. The  $K_D$  values were calculated according to equation (1) [31]:

$$\frac{1}{V_j - V_0} = \frac{1}{B_t} \left( [A]_{0,j} + y_j \right) + \frac{K_D}{B_t} \quad (1)$$

$y_j$  was calculated according to equation (2):

$$y_j = \frac{\sum_{i=1}^{j-1} ([A]_{0,i} - [A]_{0,i-1})(V_i - V_0)}{V_j - V_0} \quad (2)$$

Where  $j$  represents the  $j$ th concentration of TAM.  $V_j$  and  $[A]_{0,j}$  are the elution volume and molar concentration of TAM at the  $j$ th concentration, respectively.  $V_0$  is the elution volume of the nonspecific substance (AZT).  $y_j$  is the increased molar concentration of TAM.  $B_t$  is the total amount of immobilized MRGPRX2 receptor. A plot of  $1/V_j - V_0$  versus  $[A]_{0,j} + y_j$  should produce a linear relationship for specific system, where the  $K_D$  value can be found by taking the ratio of the intercept over the slope.

## 2.6. Competitive displacement

The competitive displacement technique is based on the interactions of different ligands with MRGPRX2 to evaluate the competitiveness of TAM towards the binding sites of the reference ligand with MRGPRX2, suggesting that they may share the same binding sites on MRGPRX2. CIP is a known MRGPRX2 agonist that employed as a reference ligand in this experiment. The CMC column (2 mm I.D.  $\times$  10 mm) was equilibrated with water (mobile phase A) for 1–2 h. Firstly, 1 mg/mL CIP was injected into the MRGPRX2-HEK293/CMC column to generate an affinity curve. After complete elution of CIP,  $1 \times 10^{-7}$  M TAM prepared in water (mobile phase B) was used to pre saturate the MRGPRX2-HEK293/CMC column. Subsequently, CIP was injected again to observe the changes of the retention time. The detection was performed at 278 nm in 37°C, with a flow rate of 0.2 mL/min.

## 2.7. Thermodynamic study

Drug-receptor interactions involve hydrogen bonding forces, van der

Waals forces, electrostatic attraction, and hydrophobic interactions [32]. The relationships of thermodynamic parameters of  $\Delta H$ ,  $\Delta S$ , and  $K_D$  value were described in the Van't Hoff equation (3) [33].

$$\ln K_D = \frac{\Delta H}{RT} - \frac{\Delta S}{R} \quad (3)$$

The  $K_D$  values were determined at different temperatures by frontal analysis [34] and the main binding forces were discussed by equation (3). The detection was performed at 238 nm in 27, 32 and 37°C, with a flow rate of 0.2 mL/min.

## 2.8. Molecular docking

SYBYL-X 2.0 software and Surflex-Dock module was used for molecular docking. MRGPRX2 protein was downloaded from PDB database (PDB ID: 7S8N). The structure of TAM was downloaded from the ChemicalBook database (CB Number: CB7853805). MRGPRX2 and TAM were optimized by Powell's method with minimized Tripos force field and Pullman charge, and assigned using Gasteiger-Hückel charges.

## 2.9. Cell viability

Cell viability of LAD2 cells, MRGPRX2-HEK293 cells or HEK293 cells were detected by CCK-8. Cells were seeded at a density of  $5 \times 10^4$  cells per well in a 96-well plate and treated with TAM, CLA, the combination of TAM and CLA, or conditioned mediums for 24 h. Then, 10  $\mu\text{L}$  of CCK-8 solution was added to each well and cultured for 2 h. OD values at 450 nm were measured using a microplate reader.

MTT assay was used to detect the cell viability of MCF-10A, MCF-7, and T-47D cells. Cells were seeded at a density of  $5 \times 10^4$  cells per well in 96-well plates and treated with TAM or conditioned mediums for 48 h. Then, culture mediums were discarded and 200  $\mu\text{L}$  of MTT solution was added to each well for 4 h incubation. The produced formazan blue was dissolved with DMSO. OD values at 490 nm were measured using a microplate reader.

## 2.10. Intracellular calcium ion ( $\text{Ca}^{2+}$ ) mobilization assay

TAM was diluted to the concentrations of 10, 20, 40  $\mu\text{M}$  in calcium imaging buffer (CIB, 125 mM NaCl, 3 mM KCl, 2.5 mM  $\text{CaCl}_2$ , 0.6 mM  $\text{MgCl}_2$ , 10 mM HEPES, 20 mM glucose, 1.2 mM  $\text{NaHCO}_3$ , 20 mM sucrose, pH 7.4). LAD2 cells, MRGPRX2-HEK293 cells, or HEK293 cells were seeded into 96-well plates in advance and cultured with incubation buffer (CIB containing 4  $\mu\text{M}$  Fluo-3 AM and 0.1% Pluronic F-127) for 30 min. Then, cells were washed and maintained with CIB in 96-well plates (50  $\mu\text{L}$ /well). At 10 s after initial imaging, TAM diluted with CIB was added to the wells. The real-time changes in calcium fluorescence intensity of LAD2 cells, MRGPRX2-HEK293 cells or HEK293 cells were monitored at 2-s intervals over 120 s, using an inverted fluorescence microscope (Nikon, Ti-U, Japan).

## 2.11. siRNA transfection of LAD2 cells and RT-PCR

MRGPRX2 knockdown was achieved using small interfering RNAs (siRNAs) targeting MRGPRX2 or a control siRNA. The following siRNA sequences were used: Negative Control siRNA, forward, 5'-UUCUCCGAACGUGUCACGUTT-3', and reverse, 5'-ACGUGACACGUUCGGAGAATT-3'; MRGPRX2 knockdown siRNA, forward, 5'-GUACAACAGUAAUGGAAATT-3', and reverse, 5'-UUUCCAUUCACUGUUGUACTT-3'. LAD2 cells were seeded at a density of  $1 \times 10^6$  cells per well in a 6-well plate and treated with transfection complex (siRNAs were delivered at a final concentration of 1  $\mu\text{M}$  with Lipofectamine® 3000 reagent in Opti-MEM medium). LAD2 cells were incubated for 48 h to allow for MRGPRX2 knockdown. RT-PCR was performed to verify the expression of MRGPRX2 mRNA using the PrimeScrip™ RT reagent kit. The following primer sequences for MRGPRX2 were used: forward: 5'-

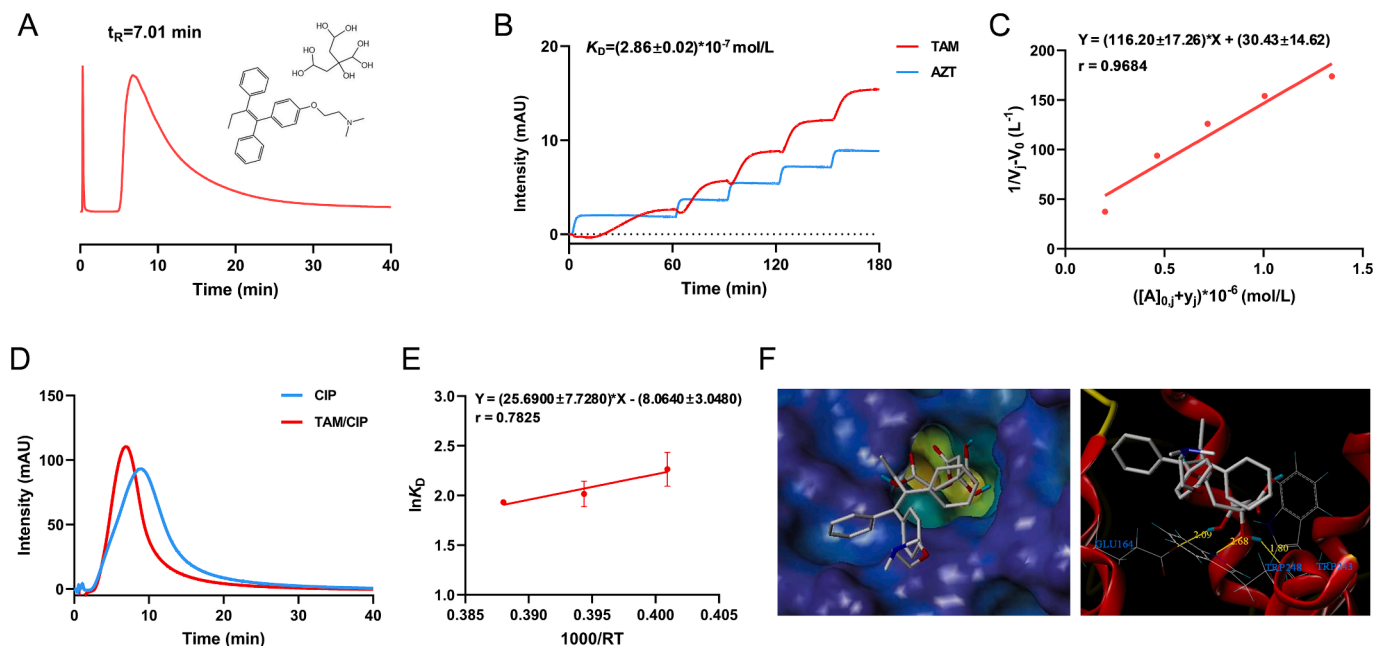


**Fig. 1.** The binding affinity of tamoxifen citrate (TAM) with mas related G protein-coupled receptor X2 (MRGPRX2). (A) Chromatogram of TAM on MRGPRX2-HEK293/CMC; (B) Breakthrough curves of TAM (red) and azidothymidine (AZT, blue), and (C) regression curve of TAM on MRGPRX2-HEK293/CMC by stepwise frontal analysis. AZT was set as negative control. The concentrations of ligands were  $2 \times 10^{-7}$ ,  $4 \times 10^{-7}$ ,  $6 \times 10^{-7}$ ,  $8 \times 10^{-7}$ , and  $1 \times 10^{-6}$  mol/L (from bottom to top), respectively; (D) Chromatograms of ciprofloxacin (CIP) before (blue) and after (red) TAM saturation on MRGPRX2-HEK293/CMC; (E) Van't Hoff regression curve of TAM binding with MRGPRX2. The  $K_D$  values at 27, 32, and 37°C were determined by frontal analysis; (F) Binding modes of TAM with MRGPRX2 by molecular docking. Experiments were performed three times.

CAGGACATTGCTGAGGTGGA-3', reverse: 5'-AGTTCAGCAAATCAGACAGACAGG-3'.

## 2.12. $\beta$ -Hexosaminidase release assay

LAD2 cells were seeded at a density of  $1 \times 10^6$  cells per well in a 96-well plate and treated with TAM (20, 40 and 80  $\mu$ M) or 30  $\mu$ g/mL of C48/80 for 30 min. The cell supernatants were subsequently collected. LAD2 cells without treatment were lysed with 0.1% Triton X-100 for the total  $\beta$ -hexosaminidase content. The  $\beta$ -hexosaminidase released into the supernatants and cell lysates were quantified by hydrolysis of *p*-nitrophenyl *N*-acetyl- $\beta$ -D-glucosamide in 0.1 M citric acid/sodium citrate buffer (10.4: 9.6, v/v) for 90 min at 37°C. 0.1 M sodium carbonate/sodium bicarbonate (9:1, v/v) was used for termination, and OD values at 405 nm were measured using a microplate reader.

## 2.13. Histamine release assay

Histamine release was measured on a HILIC column (Venusil HILIC, 2.1 mm  $\times$  150 mm, 3  $\mu$ m, Agela Technologies, Tianjin, China) by an LCMS-8040 mass spectrometer (Shimadzu Corporation, Kyoto, Japan). LAD2 cells were seeded at a density of  $1 \times 10^6$  cells per well in a 96-well plate and treated with TAM (20, 40 and 80  $\mu$ M) or 30  $\mu$ g/mL of C48/80 for 30 min. The cell supernatants were subsequently collected. 10 ng/mL of histamine-d4 as an internal standard was used for LC-ESI-MS/MS detection. Isocratic elution was performed with acetonitrile–water containing 0.1% formic acid and 20 mM ammonium formate (77:23, v/v) at a flow rate of 0.3 mL/min.

## 2.14. Cytokine and chemokine measurements

LAD2 cells were seeded at a density of  $1 \times 10^6$  cells per well in a 96-well plate and treated with TAM (20, 40 and 80  $\mu$ M) or 30  $\mu$ g/mL of C48/80 for 6 h. The cell supernatants were subsequently collected. The release of TNF- $\alpha$ , MCP-1 and IL-8 were measured by ELISA kits

according to the manufacturer's instructions.

## 2.15. Passive cutaneous anaphylaxis (PCA) assay

Male C57BL/6 mice aged 6 weeks were anesthetized with pentobarbital sodium via intraperitoneal injection. Then, 200  $\mu$ L of 0.15% Evans blue in saline was intravenously injected into each mouse. The initial thickness of the left and right hindpaw of mice were measured by vernier caliper. Next, 5  $\mu$ L of TAM (0.25, 0.5, 1.0 mg/mL) or C48/80 (30  $\mu$ g/mL) were subcutaneously injected into the left hindpaw, and an equal volume of saline was injected into the right hindpaw. After 15 min, mice were sacrificed and photos were taken later. The thickness of the hindpaws were measured again. Finally, the hindpaw were cut along foot joints, and weighted after drying. OD values of the hindpaw extracting solutions (acetone: saline, 7:3, v/v) at 630 nm were measured using a microplate reader.

## 2.16. Active systemic anaphylaxis (ASA) assay

Male C57BL/6 mice aged 6 weeks were weighted and the initial body temperatures were measured. TAM (1.265, 2.53, 5.06 mg/kg) or 30  $\mu$ g/mL C48/80 were given to the mice via tail vein injection. The equal volume of saline was injected as a control. The body temperature changes of the mice were measured at 3-min intervals over 30 min. After 6 h, mouse serums were obtained by eye blood collection.

## 2.17. Transwell migration assay

The transwell migration assay was conducted using 24-well Boyden chambers containing inserts (8.0  $\mu$ m pore size; transparent polyethylene terephthalate membrane; Corning, NY, USA). LAD2 cells with the serum-free DMEM medium were seeded at a density of  $1 \times 10^6$  cells per well in the upper chambers. The conditioned mediums of MCF-10A, MCF-7, or T-47D cells containing 20% serum were added to the lower chambers. After incubation for 48 h, the small chambers were removed.

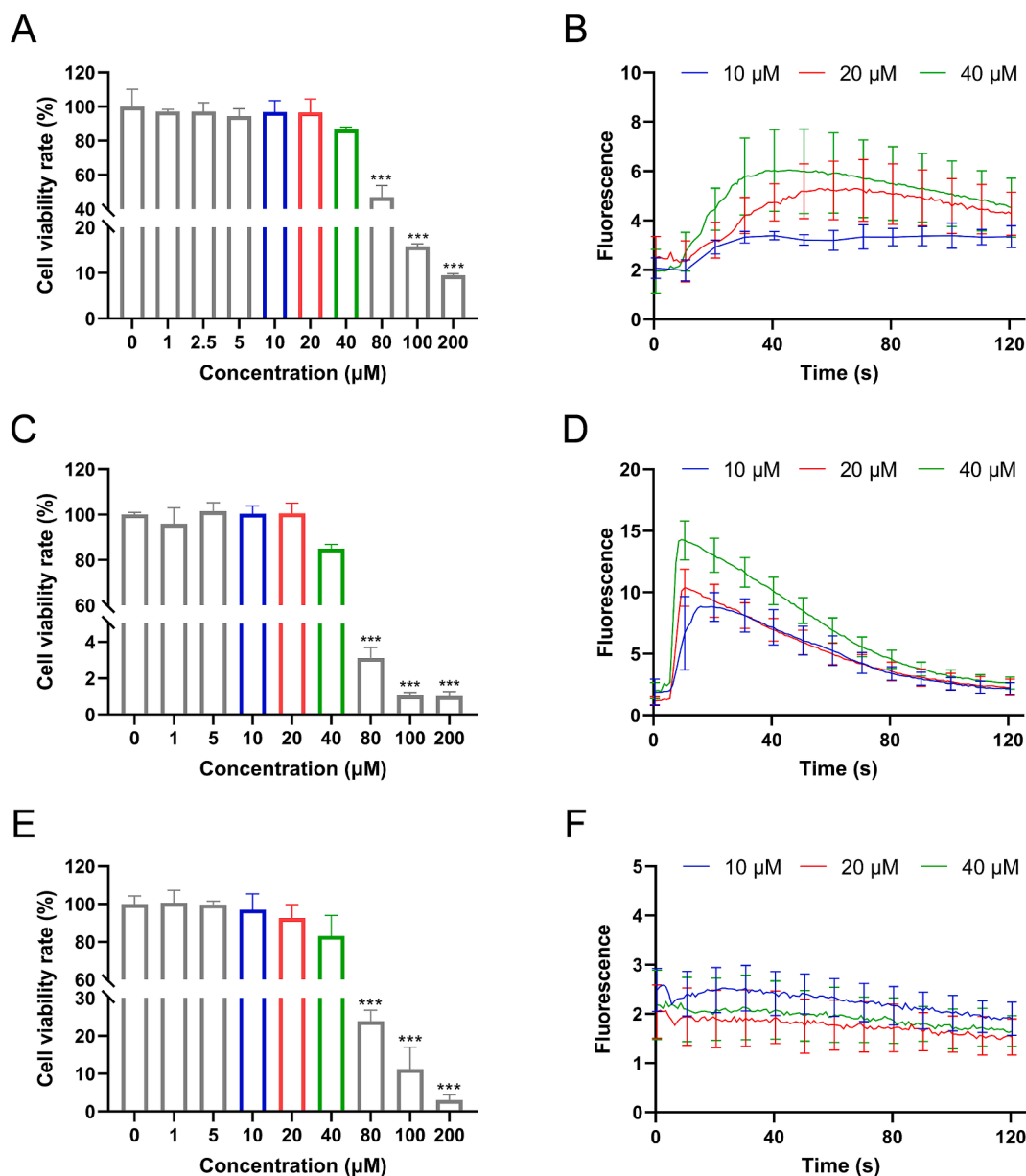


**Fig. 2.** Tamoxifen citrate (TAM) induced calcium influx of human laboratory of allergic disease 2 mast cells (LAD2 cells) and mas related G protein-coupled receptor X2-expressing HEK293 cells (MRGPRX2-HEK293 cells) *in vitro*. (A) Cell viability of LAD2 cells treated with different concentrations of TAM; (B) Calcium influx change in LAD2 cells treated with 10, 20, 40 µM TAM; (C) Cell viability of MRGPRX2-HEK293 cells treated with different concentrations of TAM; (D) Calcium influx change in MRGPRX2-HEK293 cells treated with 10, 20, 40 µM TAM; (E) Cell viability of HEK293 control cells treated with different concentrations of TAM; (F) Calcium influx change in HEK293 control cells treated with 10, 20, 40 µM TAM. Data were presented as mean ± SEM. One-way ANOVA analysis was used to determine significance in statistical comparisons. (\*\*\*)*P* < 0.001 vs. 0). Three independent experiments were performed with three samples per experiment.

LAD2 cell migration was photographed and quantified under a microscope.

**2.18. Colony formation assay**

MCF-10A and MCF-7 cells were seeded into 12-well plates in advance at a density of 50 cells per well, while T-47D cells were seeded at a density of 200 cells per well. Then, cells were incubated with conditioned mediums of LAD2 cells containing 3% serum for 48 h. Subsequently, the conditioned mediums were replaced by fresh DMEM medium. After continuous cultivation for 10 days, the colonies were fixed with 4% methanol followed by 0.5% crystal violet (Solarbio, Beijing, China) staining for 30 min. Next, the colonies were washed with PBS until the background were colorless before taking photos. Image J

software (NIH; Bethesda, MD, USA) was used to count colonies > 0.1 mm in diameter.

**2.19. Wound healing assay**

MCF-10A, MCF-7 or T-47D cells were seeded into 12-well plates and cultured until confluent. The monolayer cells were scratched with a sterile 10 µL pipette tip and were supplemented with 1 mL of DMEM medium subsequently. The scratch widths of 0 h were photographed under a microscope. Then, cells were incubated with conditioned mediums of LAD2 cells containing 3% fetal bovine serum, which were replaced by DMEM medium after 48 h to photograph the scratch widths. The migration rates were calculated by the following equation: migration rate (%) = [ (scratch widths of 0 h – scratch widths of 48 h) /

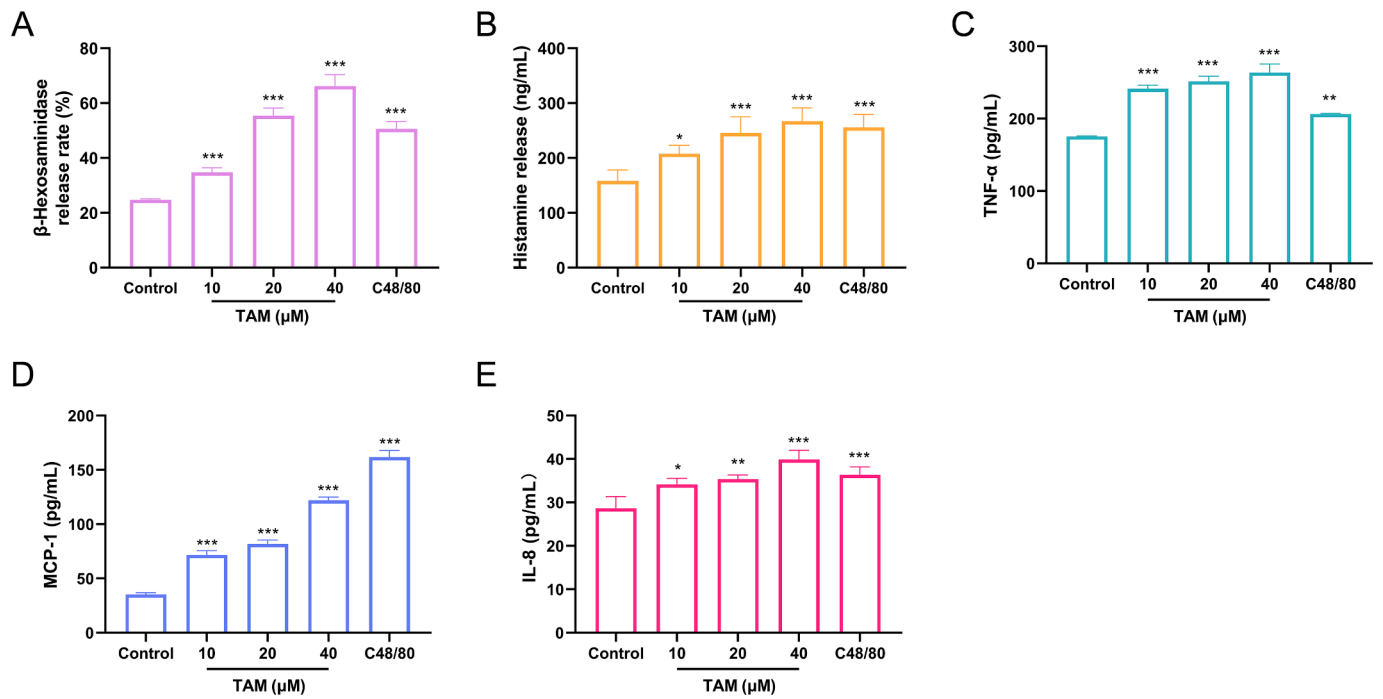


**Fig. 3. Tamoxifen citrate (TAM) induced mast cell degranulation *in vitro*.** The release of (A)  $\beta$ -hexosaminidase, (B) histamine, (C) TNF- $\alpha$ , (D) MCP-1, and (E) IL-8 from LAD2 cells treated with different concentrations of TAM. The concentrations of TAM were set as 10, 20, 40  $\mu$ M. TM buffer was set as negative control and 30  $\mu$ g/mL C48/80 as positive control. Data were presented as mean  $\pm$  SEM. One-way ANOVA analysis was used to determine significance in statistical comparisons. (\* $P < 0.05$ , \*\* $P < 0.01$ , \*\*\* $P < 0.001$  vs. Control). Three independent experiments were performed with three samples per experiment.

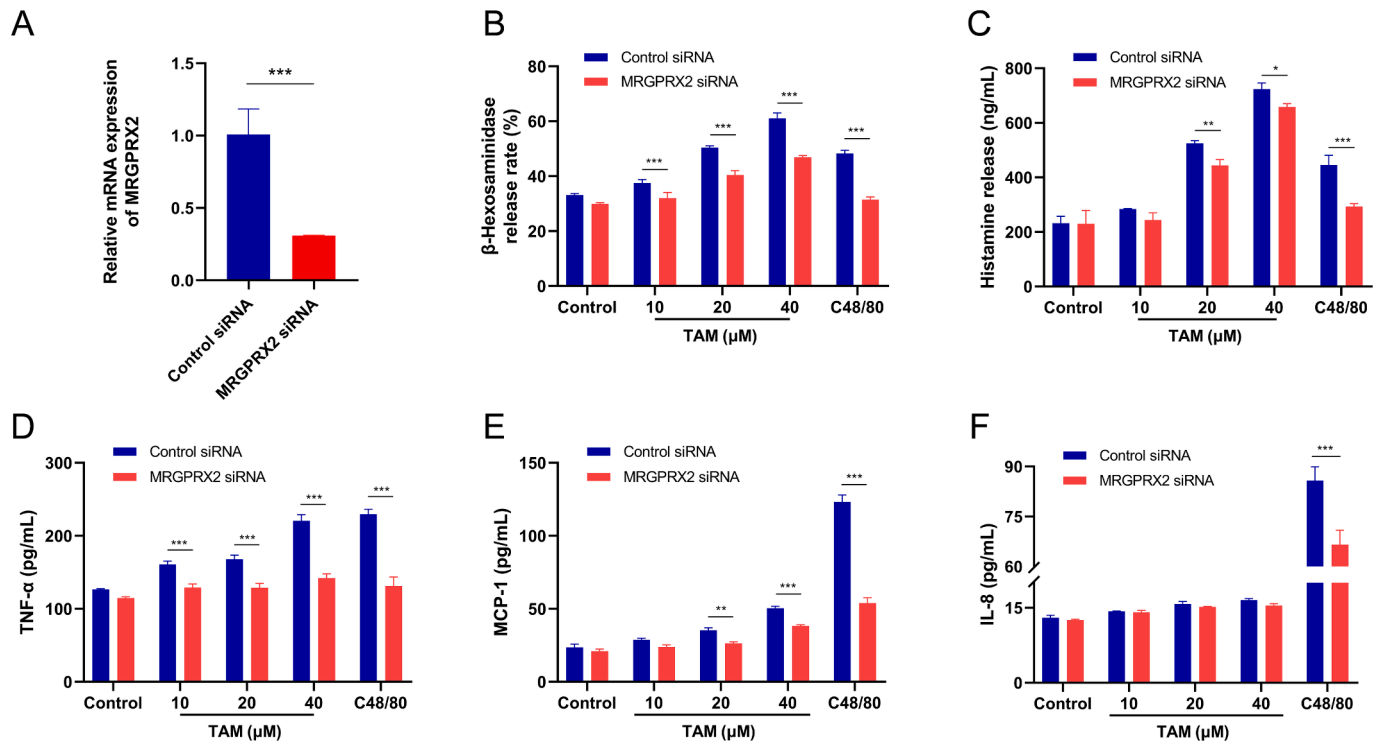


**Fig. 4. Mast cell degranulation induced by tamoxifen citrate (TAM) *in vitro* was mediated by mas related G protein-coupled receptor X2 (MRGPRX2).** (A) The relative mRNA expression of MRGPRX2 in human laboratory of allergic disease 2 mast cells (LAD2 cells) transfected with Negative Control siRNA and MRGPRX2 siRNA, respectively; The release of (B)  $\beta$ -hexosaminidase, (C) histamine, (D) TNF- $\alpha$ , (E) MCP-1, and (F) IL-8 from control LAD2 cells (Control siRNA) and MRGPRX2 knockdown LAD2 cells (MRGPRX2 siRNA) treated with different concentrations of TAM. The concentrations of TAM were set as 10, 20, 40  $\mu$ M. TM buffer was set as negative control and 30  $\mu$ g/mL C48/80 as positive control. Data were presented as mean  $\pm$  SEM. Two-way ANOVA analysis was used to determine significance in statistical comparisons. (\* $P < 0.05$ , \*\* $P < 0.01$ , \*\*\* $P < 0.001$  Control siRNA vs. MRGPRX2 siRNA). Three independent experiments were performed with three samples per experiment.

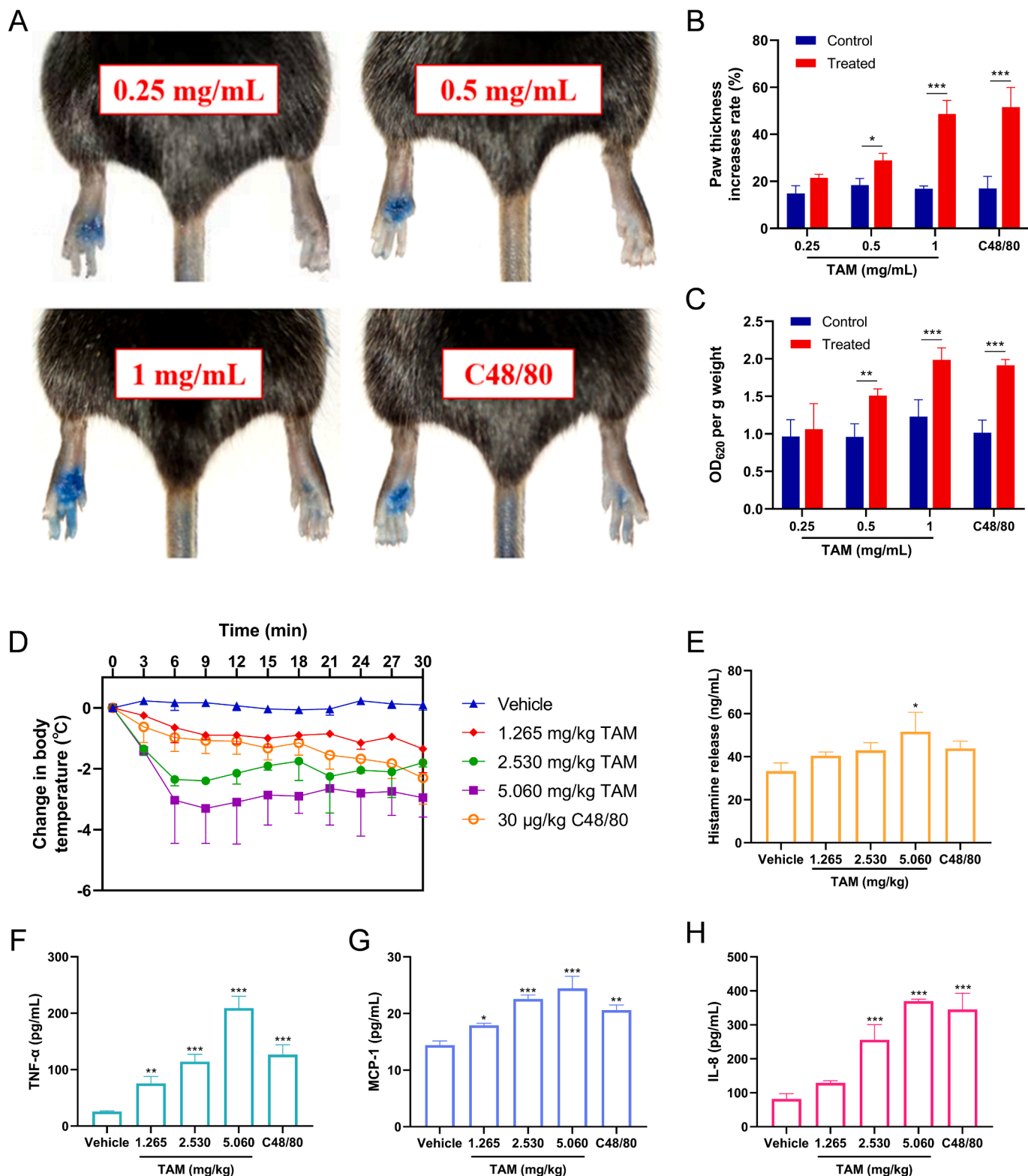


**Fig. 5. Tamoxifen citrate (TAM) induced passive cutaneous anaphylaxis (PCA) and active systemic anaphylaxis (ASA) in C57BL/6 mice.** (A) Representative images of Evans blue extravasation after intraplantar injection of TAM; The quantification of (B) paw thickness and (C) Evans blue leakage into the paw. Left paw was injected with TAM at doses of 0.25, 0.5, 1 mg/mL (Treated), while the right paw was injected with the vehicle (Control). 30 µg/mL C48/80 was set as positive control. Data were presented as mean ± SEM. Two-way ANOVA analysis was used to determine significance in statistical comparisons. (\* $P < 0.05$ , \*\* $P < 0.01$ , \*\*\* $P < 0.001$  Control vs. Treated); (D) Changes in body temperature of C57BL/6 mice after the tail vein injection with TAM; The release of (E) histamine, (F) TNF- $\alpha$ , (G) MCP-1, and (H) IL-8 from serum in C57BL/6 mice injected with different doses of TAM. The doses of TAM were set as 1.265, 2.530, 5.060 mg/kg, the same dose of vehicle was set as negative control and 30 µg/kg C48/80 as positive control. Data were presented as mean ± SEM. One-way ANOVA analysis was used to determine significance in statistical comparisons. (\* $P < 0.05$ , \*\* $P < 0.01$ , \*\*\* $P < 0.001$  vs. Vehicle). Three independent experiments were performed with three samples per experiment.

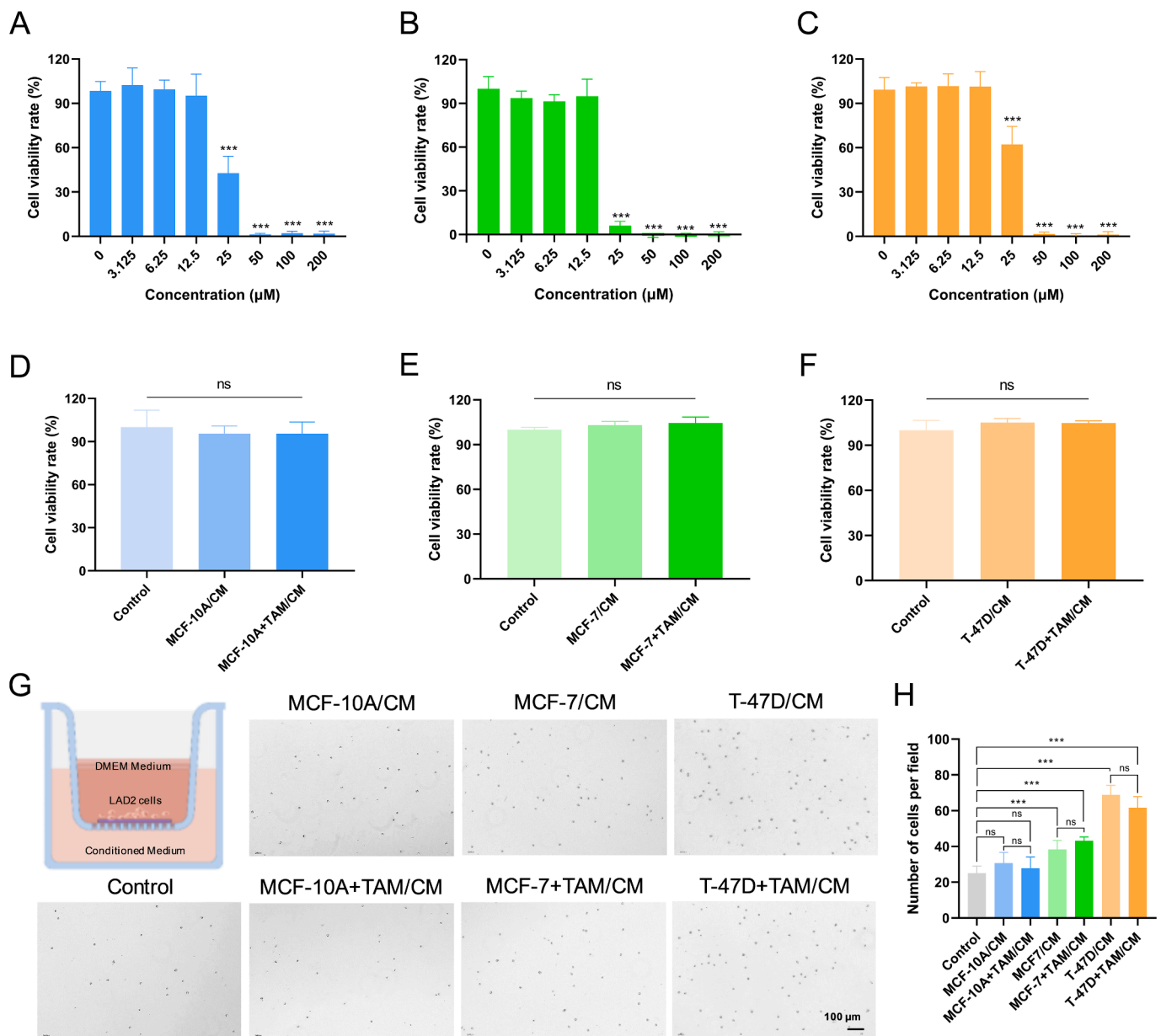


**Fig. 6. The effects of conditioned mediums (CMs) from breast cells on the proliferation and migration of human laboratory of allergic disease 2 mast cells (LAD2 cells).** Cell viability of (A) MCF-10A, (B) MCF-7, and (C) T-47D cells treated with different concentrations of tamoxifen citrate (TAM). The concentrations of TAM were set as 0, 3.125, 6.25, 12.5, 25, 50, 100, 200 μM. Data were presented as mean ± SEM. One-way ANOVA analysis was used to determine significance in statistical comparisons. (\*\*\*) $P < 0.001$  vs. 0); Cell viability of LAD2 cells in the CMs of (D) MCF-10A, (E) MCF-7, and (F) T-47D cells with or without 10 μM TAM treatment; (G) Representative images of LAD2 cell migration induced by the CMs of MCF-10A, MCF-7, and T-47D cells with or without 10 μM TAM treatment. Image scale: 100 μm; (H) The quantification of the number of migrated LAD2 cells. DMEM was set as control. Data were presented as mean ± SEM. Two-tailed unpaired student's *t*-test was used to determine significance in statistical comparisons. (\*\*\*) $P < 0.001$  vs. Control). Three independent experiments were performed with three samples per experiment.

scratch widths of 0 h] × 100%.

### 2.20. Statistical analysis

Data were expressed as the means ± SEM from three repeated experiments. Two-tailed unpaired student's *t*-test was used for comparisons between two individual groups. One-way ANOVA or two-way ANOVA analysis were used for multiple comparisons. Differences were considered significant at \* $P < 0.05$ , \*\* $P < 0.01$ , \*\*\* $P < 0.001$ .

## 3. Results

### 3.1. TAM bound specifically with MRGPRX2

MRGPRX2-HEK293/CMC model was used for the investigation of specific affinity of TAM binding with MRGPRX2. TAM bound MRGPRX2 with a retention time of 7.01 min (Fig. 1A), and gave a  $K_D$  value of  $(2.86 \pm 0.02) \times 10^{-7}$  M by stepwise frontal analysis (Fig. 1B, C). CIP, as a classic agonist of MRGPRX2 [35], was used to verify the selectivity of TAM towards MRGPRX2. After pre saturation of TAM on MRGPRX2-HEK293/CMC column, the retention time of CIP decreased and the affinity curve moved forward. This suggested that TAM was a potential agonist for

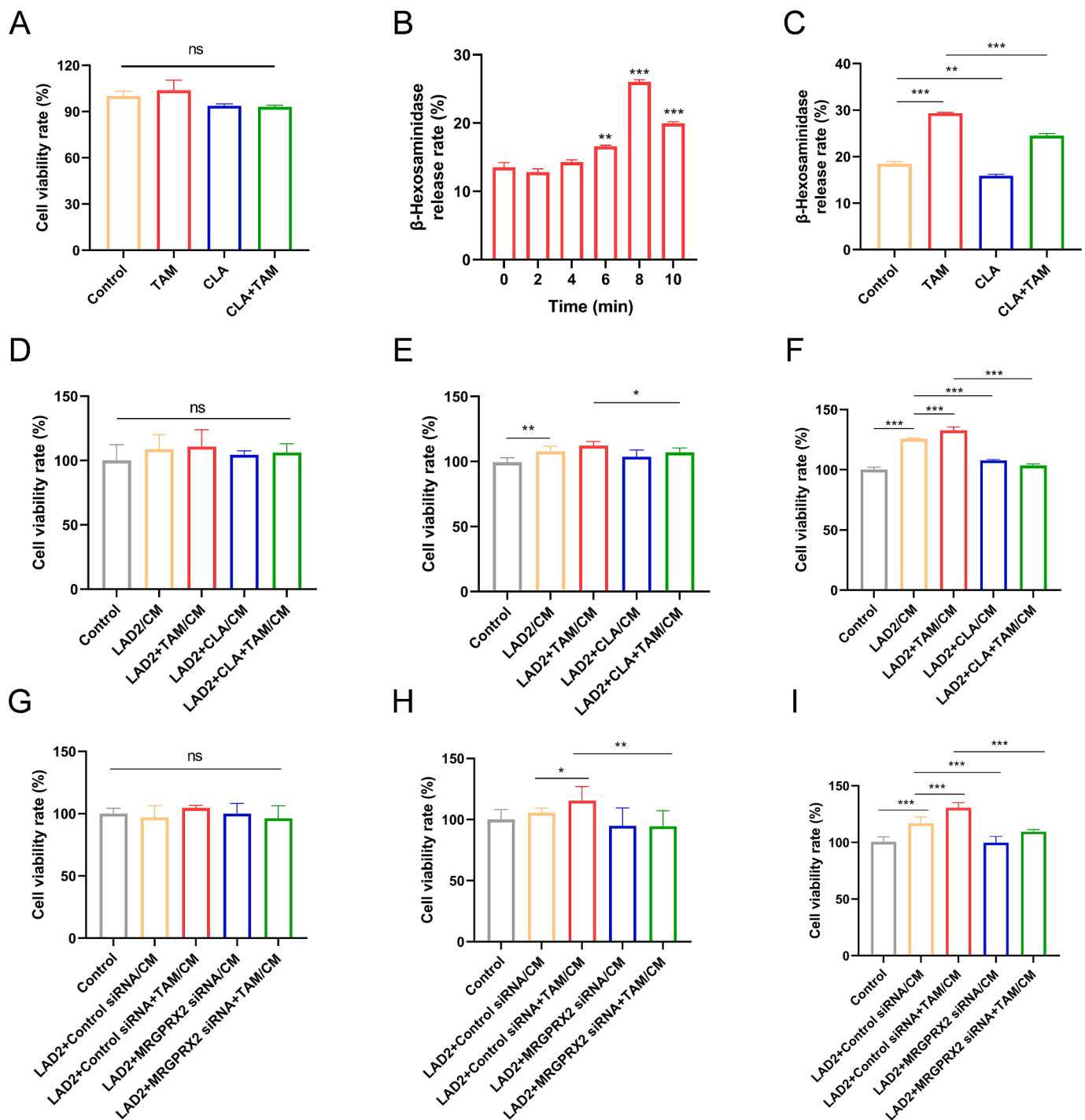


**Fig. 7. The effects of conditioned media (CMs) from human laboratory of allergic disease 2 mast cells (LAD2 cells) on the proliferation of breast cells.** (A) Cell viability of LAD2 cells with or without independent treatment of 40  $\mu$ M tamoxifen citrate (TAM), 200  $\mu$ M clarithromycin (CLA), and the combination of TAM and CLA. TM buffer was set as control; (B)  $\beta$ -Hexosaminidase release in the CMs of LAD2 cells treated with 40  $\mu$ M TAM at different times. Data were presented as mean  $\pm$  SEM. One-way ANOVA analysis was used to determine significance in statistical comparisons. (\*\* $P < 0.01$ , \*\*\* $P < 0.001$  vs. 0); (C)  $\beta$ -Hexosaminidase release in the CMs of LAD2 cells with or without independent treatment of 40  $\mu$ M TAM, 200  $\mu$ M CLA, and the combination of TAM and CLA. TM buffer was set as control; Cell viability of (D) MCF-10A, (E) MCF-7, and (F) T-47D cells in the CMs from LAD2 cells with or without independent treatment of 40  $\mu$ M TAM, 200  $\mu$ M CLA, and the combination of TAM and CLA. DMEM was set as control; Cell viability of (G) MCF-10A, (H) MCF-7, and (I) T-47D cells in the CMs from LAD2 cells with or without MRGPRX2 silencing, as well as in the presence or absence of 40  $\mu$ M TAM treatment. DMEM was set as control. Data were presented as mean  $\pm$  SEM. Two-tailed unpaired student's *t*-test was used to determine significance in statistical comparisons. (\* $P < 0.05$ , \*\* $P < 0.01$  and \*\*\* $P < 0.001$ ). Three independent experiments were performed with three samples per experiment.

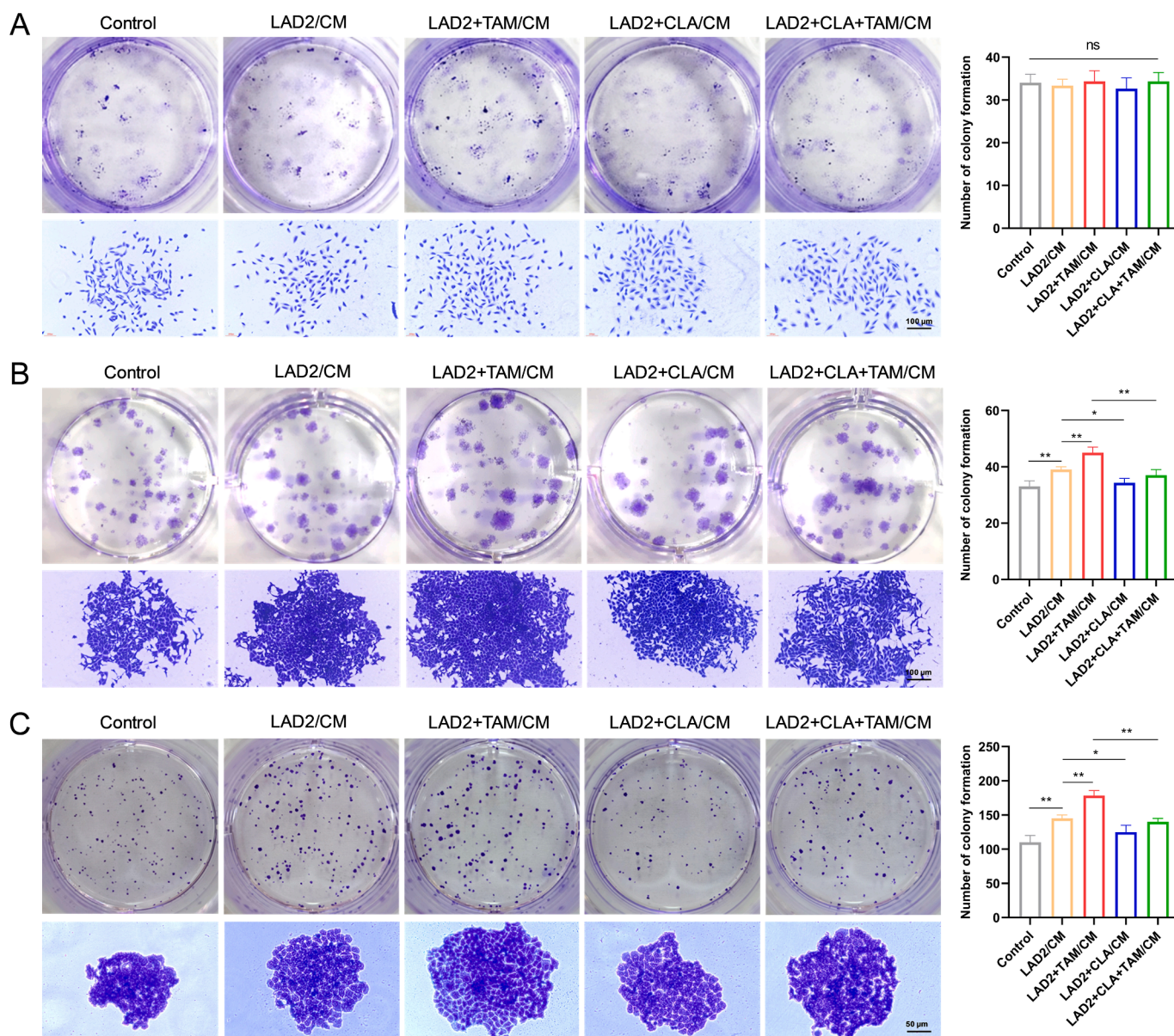


**Fig. 8.** The effects of mast cell activation induced by tamoxifen citrate (TAM) on the colony formation of breast cancer cells can be reversed by clarithromycin (CLA). Representative images and numbers of colony formation of (A) MCF-10A, (B) MCF-7, and (C) T-47D cells in the conditioned mediums (CMs) of LAD2 cells with or without independent treatment of 40  $\mu$ M TAM, 200  $\mu$ M CLA, and the combination of TAM and CLA. Image scale: 50 or 100  $\mu$ m. DMEM was set as control. Data were presented as mean  $\pm$  SEM. Two-tailed unpaired student's *t*-test was used to determine significance in statistical comparisons. (\**P* < 0.05 and \*\**P* < 0.01). Three independent experiments were performed with three samples per experiment.

MRGPRX2, as it can compete with CIP for binding to MRGPRX2 (Fig. 1D).

Furthermore, the  $K_D$  values of TAM binding with MRGPRX2 at 27, 32, and 37°C were  $(9.51 \pm 2.59) \times 10^{-7}$ ,  $(7.47 \pm 0.91) \times 10^{-7}$ , and  $(6.91 \pm 0.74) \times 10^{-7}$  M, respectively. The linear equation for Van't Hoff regression analysis between  $\ln K_D$  and  $1000/RT$  was  $y = (25.6900 \pm 7.7280) \cdot x - (8.0640 \pm 3.0480)$  (Fig. 1E). An endothermic process of TAM binding with MRGPRX2 was confirmed by  $\Delta H > 0$  and  $\Delta S > 0$ , according to the thermodynamic principles of chemical reactions [33]. This proved that hydrophobic forces were the main driving force for TAM binding with MRGPRX2. In addition, TAM can form three hydrogen bonds with residues of TRP243, TRP248, and GLU164 in MRGPRX2 by molecular docking (Fig. 1F).

### 3.2. TAM induced mast cell activation via MRGPRX2

Mast cell activation was detected by calcium mobilization and degranulation. LAD2 cell viability was more than 80% within concentrations of 40  $\mu$ M TAM (Fig. 2A). Calcium imaging of LAD2 cells showed a strongly activated response effect, which was produced by TAM at concentrations of 10, 20, 40  $\mu$ M (Fig. 2B). MRGPRX2-HEK293 cells were used to assess the contribution of MRGPRX2 in mast cell calcium mobilization, with HEK 293 control cells serving as a control. TAM did not significantly affect cell viability at concentrations below 40  $\mu$ M (Fig. 2C, E). The intracellular  $Ca^{2+}$  concentrations of MRGPRX2-HEK293 cells were increased by TAM in a dose-dependent manner (Fig. 2D), while TAM rarely affected  $Ca^{2+}$  influx change in HEK293 control cells (Fig. 2F). It was indicated that TAM induced mast cell calcium mobilization via MRGPRX2.

Calcium influx change shows a subsequent effect on mast cell

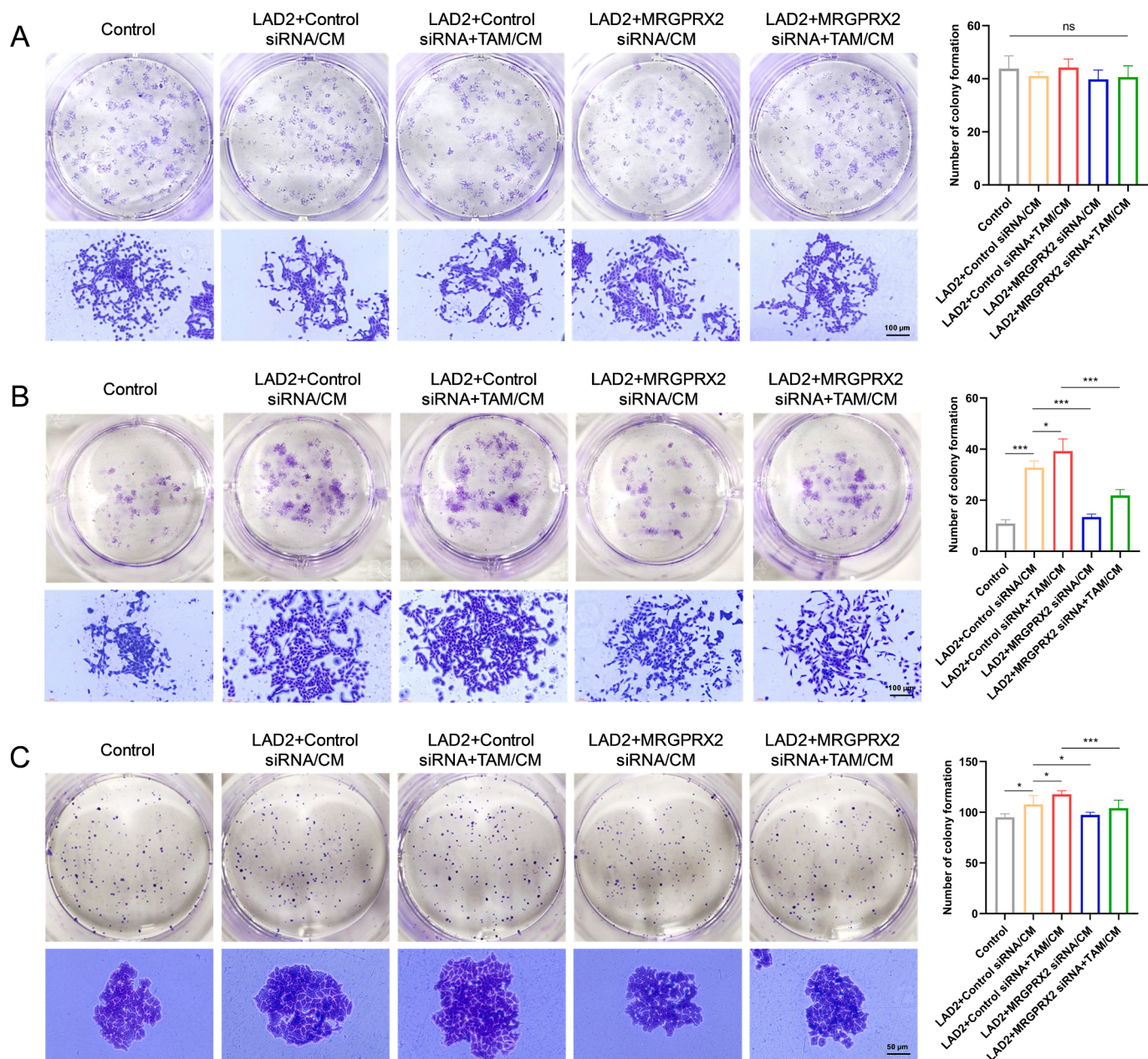


**Fig. 9.** The effects of mast cell activation induced by tamoxifen citrate (TAM) on the colony formation of breast cancer cells can be reversed by mast cell related G protein-coupled receptor X2 (MRGPRX2) silencing. Representative images and numbers of colony formation of (A) MCF-10A, (B) MCF-7, and (C) T-47D cells in the conditioned mediums (CMs) of LAD2 cells with or without MRGPRX2 knockdown, as well as in the presence or absence of 40  $\mu$ M TAM treatment. Image scale: 50 or 100  $\mu$ m. DMEM was set as control. Data were presented as mean  $\pm$  SEM. Two-tailed unpaired student's *t*-test was used to determine significance in statistical comparisons. (\**P* < 0.05 and \*\*\**P* < 0.001). Three independent experiments were performed with three samples per experiment.

degranulation, which includes the rapid secretion of pre-formed inflammatory mediators and synthetic cytokines [36]. C48/80 is a specific MRGPRX2 agonist used as positive control. TAM dose-dependently increased the release of  $\beta$ -hexosaminidase, histamine, TNF- $\alpha$ , MCP-1 and IL-8 in LAD2 cells (Fig. 3). Besides, MRGPRX2 was knocked down through siRNA interference of LAD2 cells (Fig. 4A). The release of  $\beta$ -hexosaminidase, histamine, TNF- $\alpha$ , and MCP-1 induced by TAM were significantly weakened in MRGPRX2 knockdown LAD2 cells, compared to control LAD2 cells (Fig. 4B-F). It was confirmed that MRGPRX2 mediated mast cell degranulation induced by TAM.

### 3.3. TAM induced pseudo-allergic reactions in C57BL/6 mice

PCA mouse models were used to explore the *in vivo* pseudo-allergic

reactions induced by TAM. TAM produced a dose-dependent increase in swelling and Evans blue extravasation of the left hindpaw, compared to right hindpaw that injected with physiological saline (Fig. 5A-C). It was revealed that TAM could induce local pseudo-allergic reactions in C57BL/6 mice.

Furthermore, different doses of TAM were intravenously injected into C57BL/6 mice, and body temperature changes within 30 min were monitored to investigate ASA induced by TAM. TAM caused dose-dependently rapid decreases in body temperature of the mice, which maintained at low levels for a period of time. The degrees of temperature decrease induced by TAM at doses of 2.530 and 5.060 mg/kg were higher than that induced by C48/80 (Fig. 5D). Besides, mouse serums treated with TAM for 6 h were collected. The release of histamine, TNF- $\alpha$ , MCP-1, and IL-8 in serum increased remarkably by TAM in a dose

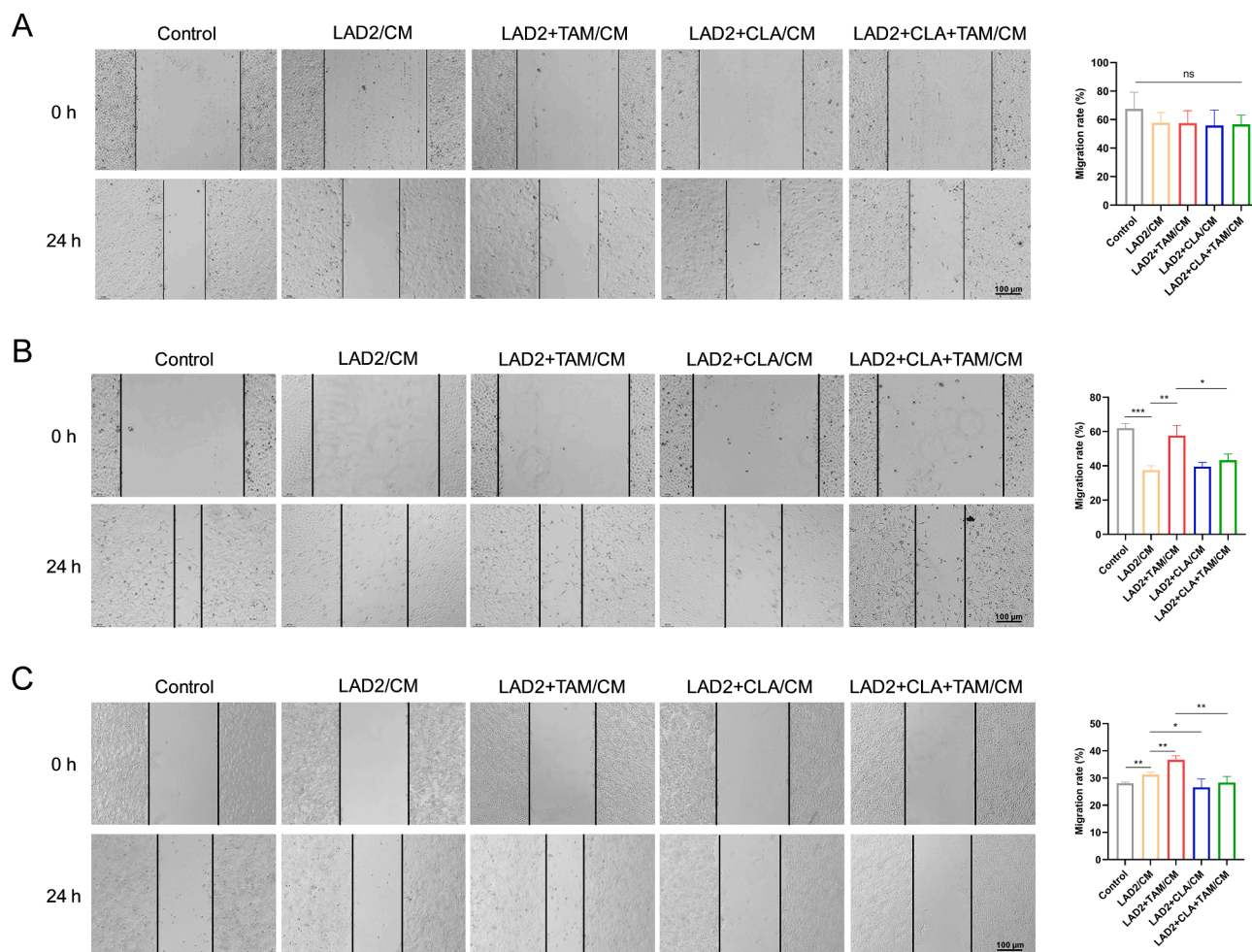


**Fig. 10.** The effects of mast cell activation induced by tamoxifen citrate (TAM) on the migration of breast cancer cells can be reversed by clarithromycin (CLA). Representative images and migration rates of wound healing of (A) MCF-10A, (B) MCF-7, and (C) T-47D cells in the conditioned mediums (CMs) of LAD2 cells with or without independent treatment of 40  $\mu$ M TAM, 200  $\mu$ M CLA, and the combination of TAM and CLA. Image scale: 100  $\mu$ m. DMEM was set as control. Data were presented as mean  $\pm$  SEM. Two-tailed unpaired student's *t*-test was used to determine significance in statistical comparisons. (\* $P$  < 0.05, \*\* $P$  < 0.01 and \*\*\* $P$  < 0.001). Three independent experiments were performed with three samples per experiment.

dependent manner (Fig. 5E-H), which were consistent with the results *in vitro* (Fig. 3).

### 3.4. Breast cancer cells could recruit mast cells

Human noncancerous breast cell line (MCF-10A) and human breast cancer cell lines (MCF-7 and T-47D) were used to investigate the interaction between LAD2 cells and breast cancer cells. The conditioned mediums of MCF-10A, MCF-7, and T-47D cells with or without TAM treatment were used for indirect cocultures of LAD2 cells. The cytotoxicity of TAM on MCF-10A, MCF-7 and T-47D cells were first evaluated. Cell viability of MCF-10A, MCF-7 and T-47D cells were not significantly affected by TAM at concentrations below 12.5  $\mu$ M (Fig. 6A-C). Therefore, 10  $\mu$ M of TAM was selected for the collection of the conditioned mediums from breast cells.

The conditioned mediums of MCF-10A, MCF-7, or T-47D cells did not affect the proliferation of LAD2 cells (Fig. 6D-F). Meanwhile, conditioned mediums of MCF-10A cells did not significantly promote the migration of LAD2 cells by transwell assay. However, conditioned mediums from both MCF-7 and T-47D cells significantly induced LAD2 cell migration to the lower chamber. Interestingly, additional TAM treatment had no significant effect on the LAD2 cell migration induced by conditioned mediums of MCF-7 and T-47D cells (Fig. 6G, H). This indicated that ER<sup>+</sup> breast cancer cells could recruit mast cells to participate the

composition of breast cancer microenvironment.

### 3.5. Mast cell activation induced by TAM promoted the proliferation and migration of breast cancer cells

CLA has been reported as an MRGPRX2 antagonist that inhibits mast cell activation, as well as a mast cell membrane stabilizer for anti-inflammatory and anti-allergic purposes [37,38]. The conditioned mediums of LAD2 cells with or without independent treatment of 40  $\mu$ M TAM, 200  $\mu$ M CLA, or the combination of TAM and CLA were used for indirect cocultures of MCF-10A, MCF-7, and T-47D cells. Cell viability of LAD2 cells were not significantly affected by independent or combinational treatment of 40  $\mu$ M TAM and 200  $\mu$ M CLA (Fig. 7A).  $\beta$ -Hexosaminidase release assay was used to determine the optimal stimulation time of TAM in the collection of conditioned mediums from LAD2 cells. The highest content of  $\beta$ -hexosaminidase in conditioned mediums of LAD2 cells was observed in TAM treatment for 8 min (Fig. 7B). TAM increased  $\beta$ -hexosaminidase release in conditioned mediums of LAD2 cells, while CLA decreased it significantly. Notably, CLA significantly reversed the increased  $\beta$ -hexosaminidase release of LAD2 cells induced by TAM (Fig. 7C), which indicated that CLA could inhibit TAM-induced mast cell activation.

The conditioned mediums of LAD2 cells did not affect the proliferation of MCF-10A cells (Fig. 7D). However, for ER<sup>+</sup> breast cancer cells,

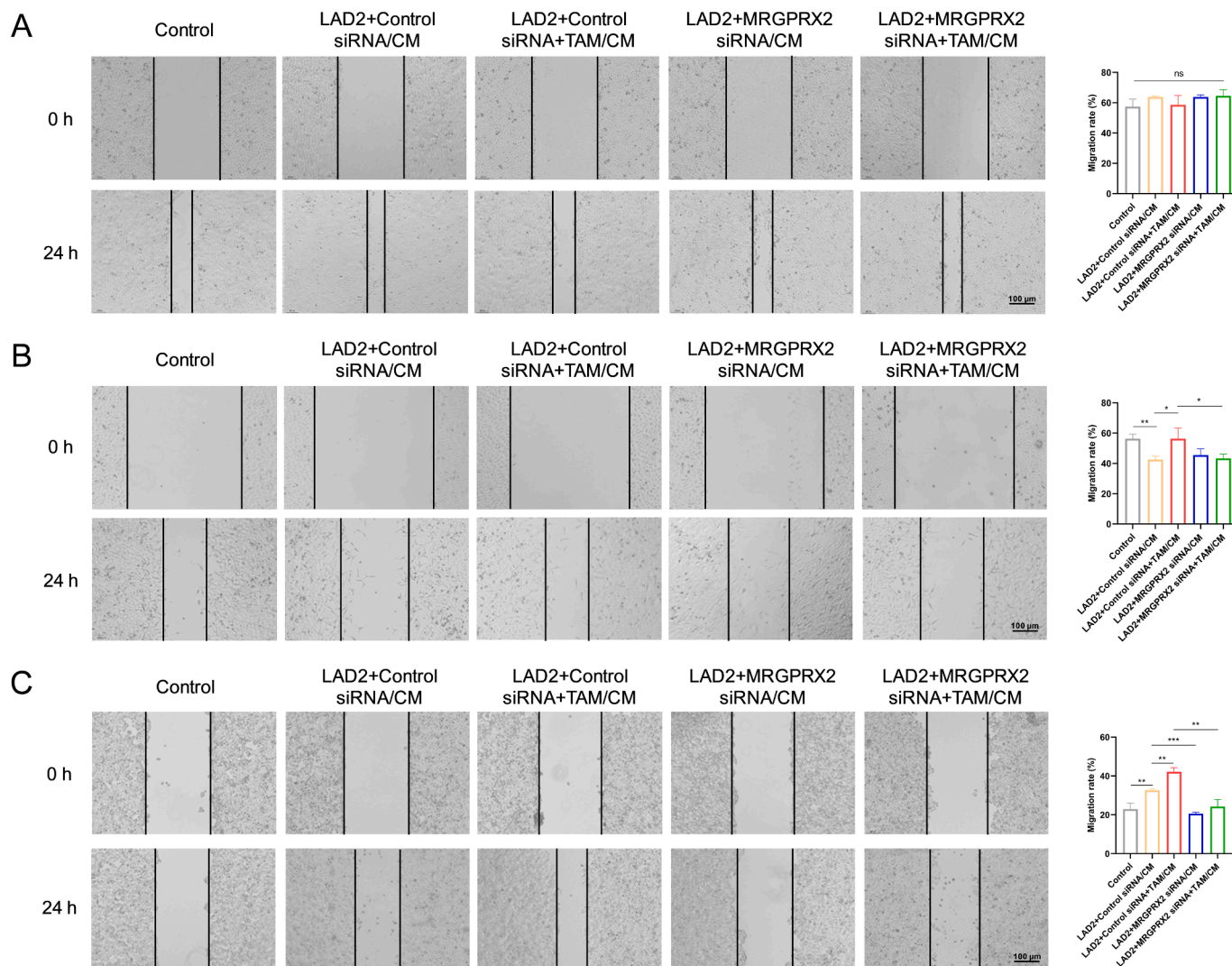


**Fig. 11.** The effects of mast cell activation induced by tamoxifen citrate (TAM) on the migration of breast cancer cells can be reversed by mas related G protein-coupled receptor X2 (MRGPRX2) silencing. Representative images and migration rates of wound healing of (A) MCF-10A, (B) MCF-7, and (C) T-47D cells in the conditioned mediums (CMs) of LAD2 cells with or without MRGPRX2 knockdown, as well as in the presence or absence of 40  $\mu$ M TAM treatment. Image scale: 100  $\mu$ m. DMEM was set as control. Data were presented as mean  $\pm$  SEM. Two-tailed unpaired student's *t*-test was used to determine significance in statistical comparisons. (\**P* < 0.05, \*\**P* < 0.01 and \*\*\**P* < 0.001). Three independent experiments were performed with three samples per experiment.

conditioned mediums of LAD2 cells promoted the proliferation of MCF-7 and T-47D cells, which were further enhanced by additional TAM treatment. Meanwhile, additional CLA treatment had no significant effect on the proliferation of MCF-7 cells, while inhibited the proliferation of T-47D cells, compared with conditioned mediums of LAD2 cells. Moreover, CLA could significantly reverse the proliferation promotion of MCF-7 and T-47D cells by inhibiting TAM-induced mast cell activation (Fig. 7E, F). Additionally, MRGPRX2 was silenced using siRNA interference in LAD2 cells. The conditioned mediums from LAD2 cells with MRGPRX2 siRNA interference exhibited effects on the proliferation of these three cell lines that were similar to those observed with CLA (Fig. 7G-I).

The conditioned mediums of LAD2 cells did not affect the number and size of MCF-10A cell colonies (Fig. 8A). However, conditioned mediums of LAD2 cells significantly promoted the colony formation of MCF-7 and T-47D cells, which were further enhanced by additional TAM treatment, but inhibited by additional CLA treatment reversely. Moreover, CLA could effectively reverse the enhanced colony formation of MCF-7 and T-47D cells caused by TAM-induced mast cell activation (Fig. 8B, C). Meanwhile, MRGPRX2 silencing exhibited comparable effects on the colony formation of MCF-7 and T-47D cells, as using

MRGPRX2 antagonist CLA (Fig. 9).

The conditioned mediums of LAD2 cells did not affect the migration of MCF-10A cells (Fig. 10A). Interestingly, conditioned mediums of LAD2 cells significantly promoted the migration of T-47D cells, but inhibited the migration of MCF-7 cells, both of which were further promoted by additional TAM treatment. It was speculated that the genotype expression of MCF-7 and T-47D cells affected their migration behavior mediated by mast cells. Compared with conditioned mediums of LAD2 cells, additional CLA treatment did not affect the migration of MCF-7 cells, while significantly inhibited the migration of T-47D cells. Moreover, CLA could effectively reverse the enhanced migration abilities of MCF-7 and T-47D cells caused by TAM-induced mast cell activation (Fig. 10B, C). It was noteworthy that MRGPRX2 silencing produced effects similar to those of CLA (Fig. 11).

#### 4. Discussion

Chemotherapy is one of the most effective means for cancer therapy, which mainly affects the life activities of tumor cells by interfering with the biosynthesis of nucleic acids and the structure and function of proteins, or disrupting hormone balance [39]. Allergic reactions have been

reported in the vast majority of chemotherapy drugs due to the high toxicity and irritancy [40,41]. Although the overall incidence rate is not high, the consequences are very serious [42]. Therefore, the investigation of potential sensitization in chemotherapy drugs is of great practical significance for clinical guidance on safe medication and improvement of the quality of cancer patients lives.

Allergic reactions were involved in the rare adverse reactions of TAM in clinical treatment for breast cancer, which we speculated that MRGPRX2 was the target receptor. In our study, TAM can specifically bind to MRGPRX2 with a  $K_D$  value of  $(2.86 \pm 0.02) \times 10^{-7}$  M. Calcium mobilization was the first step to trigger mast cell degranulation [36]. TAM was found to induce calcium influx in LAD2 cells mediated by MRGPRX2. The release of  $\beta$ -hexosaminidase (a marker protein highly associated with inflammation), histamine (a classic endogenous itch substance), TNF- $\alpha$  and MCP-1 (pro-inflammatory cytokines with chemotaxis of various inflammatory cells), and IL-8 (a neutrophil chemotactic factor and an important indicator for allergic reactions) [43,44] were increased by TAM *in vitro* and *in vivo*. Moreover, TAM could induce pseudo-allergic reactions *in vivo*. It was suggested that MRGPRX2 was the key target receptor for allergic reactions in TAM treatment for breast cancer.

The recruitment of mast cells by tumor cells can intervene in tumor progression, by altering the tumor microenvironment [25]. In our study, ER<sup>+</sup> breast cancer cells can recruit mast cells into the adjacent tissues, and mast cell activation induced by TAM promoted the proliferation and migration of ER<sup>+</sup> breast cancer cells. To some extent, mast cell activation in TAM treatment for breast cancer tend to have potential adverse effects on breast cancer, which should be a comprehensive responses of inflammatory mediators released by mast cells. Further study needed to determine the specific effects of inflammatory mediators involved. Moreover, this adverse effects can be reversed by an MRGPRX2 antagonist CLA and MRGPRX2 silencing [37]. It was suggested that the potential of MRGPRX2 as an adjunctive target for breast cancer treatment.

MRGPRX2 is a member of the G protein-coupled receptor family predominantly expressed in sensory neurons, mast cells, and keratinocytes [12]. It is located in adipose tissue, esophagus, bladder, and lungs, with the highest levels found in the skin [45]. Some exogenous substances—such as C48/80, ant venom peptides, and specific drugs (neuromuscular blockers, fluoroquinolones, vancomycin)—can activate mast cells via MRGPRX2 to induce allergic reactions [35]. Notably, several endogenous peptides—including substance P, cathelicidin LL-37, PAMP-12, and vasoactive intestinal peptide—also acting as MRGPRX2 agonists [45–47].

Specifically, substance P is an endogenous neuropeptide that is widely distributed in the central and peripheral nervous systems, and immune system of mammals. Substance P/neurokinin 1 receptor mediates a range of biological effects, including pain, inflammation, immune regulation [48]; It also promotes the proliferation, invasion, metastasis, and angiogenesis of tumors [49]. Notably elevated levels of substance P have been identified across multiple human cancer tissues [50]. It was detected in the cytoplasm and nucleus of cancerous cells, as well as in the tumor body and adjacent tissues [51,52]. Importantly, substance P arose from the degradation of protachykinin A, whose levels were significantly elevated in breast cancer cells compared to normal breast epithelial cells [53]. Moreover, Davoodian et al. reported that serum levels of substance P were markedly higher among breast cancer patients than those observed in healthy individuals [54]. In addition, the expression of cathelicidin LL-37 in breast cancer cells was significantly increased, which exhibited a positive correlation with malignancy severity [55].

The presence or significant increase of endogenous MRGPRX2 agonists around the tumor tissues or at the systemic level suggested that, we should pay more attention to the potential adverse effects of MRGPRX2 activation in mast cells on breast cancer, as those observed with TAM. Given the reported high expression of substance P and cathelicidin LL-37 across multiple tumor types [50,56], further research warrants to

elucidate the precise effects of MRGPRX2 activation on different tumors and to uncover the underlying mechanisms involved.

In conclusion, our study introduced a novel anti-allergic therapeutic strategy to improve TAM treatment for ER<sup>+</sup> breast cancer, and preliminarily confirmed that mast cell activation induced by TAM via MRGPRX2 played a potential adverse role in breast cancer. However, further detailed investigation into the specific mechanisms and the *in vivo* validation are necessary. Clarifying the role of MRGPRX2 in cancer immunity and tumor therapy remains a considerable challenge ahead. The future use of mast cell membrane stabilizers or MRGPRX2 antagonists could serve as a promising adjunctive option for cancer therapy.

#### CRedit authorship contribution statement

**Jiapan Gao:** Writing – original draft, Methodology, Investigation. **Xinyue Su:** Methodology, Investigation. **Yuxiu Zhang:** Formal analysis, Data curation. **Xiaoyu Ma:** Formal analysis, Data curation. **Bingxi Ren:** Visualization, Validation. **Panpan Lei:** Visualization, Validation. **Jinming Jin:** Methodology, Formal analysis. **Weina Ma:** Writing – review & editing, Supervision, Conceptualization.

#### Declaration of competing interest

The authors declare that they have no known competing financial interests or personal relationships that could have appeared to influence the work reported in this paper.

#### Acknowledgements

This work was supported by National Natural Science Foundation of China [grant numbers 82150201, 81930096].

#### Data availability

Data will be made available on request.

#### References

- [1] R.L. Siegel, A.N. Giaquinto, A. Jemal, Cancer statistics, 2024, *CA Cancer J Clin* 74 (1) (2024) 12–49, <https://doi.org/10.3322/caac.21820>.
- [2] A.J. Kerr, D. Dodwell, P. McGale, F. Holt, F. Duane, G. Mannu, S.C. Darby, C. W. Taylor, Adjuvant and neoadjuvant breast cancer treatments: A systematic review of their effects on mortality, *Cancer Treat Rev* 105 (2022) 102375, <https://doi.org/10.1016/j.ctrv.2022.102375>.
- [3] W.H. Zhou, Y.W. Jiang, Y.Q. Xu, Y.H. Wang, X.W. Ma, L.H. Zhou, Y.P. Lin, Y. Wang, Z.P. Wu, M. Li, W.J. Yin, J.S. Lu, Comparison of adverse drug reactions between tamoxifen and toremifene in breast cancer patients with different CYP2D6 genotypes: A propensity-score matched cohort study, *Int J Cancer* 150 (10) (2022) 1664–1676. <https://doi.org/10.1002/ijc.33919>.
- [4] R. Mofarrah, R. Mofarrah, B. Kränke, M. Rahmani, K. Jahani Amiri, M. Ghasemi, N. Jallab, S. Ghobadiaski, N. Rahmani, N. Hashemi, First report of tamoxifen-induced baboon syndrome, *J Cosmet Dermatol* 20 (8) (2021) 2574–2578. <https://doi.org/10.1111/jocd.13863>.
- [5] U. Kulkarni, V. Nayak, M.M. Prabhu, R. Rao, Tamoxifen-induced vasculitis, *J Oncol Pharm Pract* 26 (3) (2020) 735–737, <https://doi.org/10.1177/1078155219862342>.
- [6] A.R. Pinto, F. Carolino, Exploring the relationship between tamoxifen and hereditary angioedema, *Eur J Breast Health* 20 (1) (2023) 71–72, <https://doi.org/10.4274/ejbh.galenos.2023.2023-12-9>.
- [7] G. Yang, S. Nowshheen, K. Aziz, A.G. Georgakilas, Toxicity and adverse effects of tamoxifen and other anti-estrogen drugs, *Pharmacol Ther* 139 (3) (2013) 392–404, <https://doi.org/10.1016/j.pharmthera.2013.05.005>.
- [8] M. Babina, S. Guhl, M. Artuc, T. Zuberbier, Allergic Fc $\epsilon$ RI- and pseudo-allergic MRGPRX2-triggered mast cell activation routes are independent and inversely regulated by SCF, *Allergy* 73 (1) (2018) 256–260, <https://doi.org/10.1111/all.13301>.
- [9] D.P. Potaczek, M. Kabisch, Current concepts of IgE regulation and impact of genetic determinants, *Clin Exp Allergy* 42 (6) (2012) 852–871, <https://doi.org/10.1111/j.1365-2222.2011.03953.x>.
- [10] M. Babina, F. Kirn, D. Hoser, D. Ernst, W. Rohde, T. Zuberbier, M. Worm, Tamoxifen counteracts the allergic immune response and improves allergen-induced dermatitis in mice, *Clin Exp Allergy* 40 (8) (2010) 1256–1265, <https://doi.org/10.1111/j.1365-2222.2010.03472.x>.

- [11] S. Roy, C. Chompunud Na Ayudhya, M. Thapaliya, V. Deepak, H. Ali, Multifaceted MRGPRX2: New insight into the role of mast cells in health and disease, *J Allergy Clin Immunol* 148 (2) (2021) 293–308. <https://doi.org/10.1016/j.jaci.2021.03.049>.
- [12] B.D. McNeil, P. Pundir, S. Meeker, L. Han, B.J. Udem, M. Kulka, X. Dong, Identification of a mast-cell-specific receptor crucial for pseudo-allergic drug reactions, *Nature* 519 (7542) (2015) 237–241. <https://doi.org/10.1038/nature14022>.
- [13] K. Lansu, J. Karpiak, J. Liu, X.P. Huang, J.D. McCorvy, W.K. Kroeze, T. Che, H. Nagase, F.I. Carroll, J. Jin, B.K. Shoichet, B.L. Roth, In silico design of novel probes for the atypical opioid receptor MRGPRX2, *Nat Chem Biol* 13 (5) (2017) 529–536. <https://doi.org/10.1038/nchembio.2334>.
- [14] D.L. Che, J. Wang, Y.Y. Ding, R. Liu, J. Cao, Y.J. Zhang, Y.J. Hou, H.L. An, Z.J. Gao, T. Zhang, Mivacurium induce mast cell activation and pseudo-allergic reactions via MAS-related G protein coupled receptor-X2, *Cell Immunol* 332 (2018) 121–128. <https://doi.org/10.1016/j.cellimm.2018.08.005>.
- [15] T. Zhang, D.L. Che, R. Liu, S.L. Han, N. Wang, Y.Z. Zhan, P. Pundir, J. Cao, Y.N. Lv, L. Yang, J. Wang, M.W. Ding, X.Z. Dong, L.C. He, Typical antimicrobials induce mast cell degranulation and anaphylactoid reactions via MRGPRX2 and its murine homologue MRGPRB2, *Eur J Immunol* 47 (11) (2017) 1949–1958. <https://doi.org/10.1002/eji.201746951>.
- [16] R. Liu, D.L. Che, T.T. Zhao, P. Pundir, J. Cao, Y.N. Lv, J. Wang, P.Y. Ma, J. Fu, N. Wang, X.Y. Wang, T. Zhang, X.Z. Dong, L.C. He, MRGPRX2 is essential for sinomenine hydrochloride induced anaphylactoid reactions, *Biochem Pharmacol* 146 (2017) 214–223. <https://doi.org/10.1016/j.bcp.2017.09.017>.
- [17] T. Zhang, R. Liu, D.L. Che, P. Pundir, N. Wang, S.L. Han, J. Cao, Y.N. Lv, H.Y. Dong, F. Fang, J. Wang, P.Y. Ma, T.T. Zhao, T. Lei, X.Z. Dong, L.C. He, A mast cell-specific receptor is critical for granuloma induced by intrathecal morphine infusion, *J Immunol* 203 (7) (2019) 1701–1714. <https://doi.org/10.4049/jimmunol.1801423>.
- [18] P.M. Mertes, F. Alla, P. Tréchet, Y. Auroy, E. Jouglu, Groupe d'Etudes des Réactions Anaphylactoides Peranesthésiques, Anaphylaxis during anesthesia in France: An 8-year national survey, *J Allergy Clin Immunol* 128 (2) (2011) 366–373. <https://doi.org/10.1016/j.jaci.2011.03.003>.
- [19] W. Koppert, J.A. Blunk, L.J. Petersen, P. Skov, K. Rentsch, M. Schmelz, Different patterns of mast cell activation by muscle relaxants in human skin, *Anesthesiology* 95 (3) (2001) 659–667. <https://doi.org/10.1097/0000542-200109000-00019>.
- [20] H. Ali, Emerging roles for MAS-Related G Protein-coupled Receptor-X2 in host defense peptide, opioid, and neuroepitide-mediated inflammatory reactions, *Adv Immunol* 136 (2017) 123–162. <https://doi.org/10.1016/bs.ai.2017.06.002>.
- [21] D. Fujisawa, J. Kashiwakura, H. Kita, Y. Kikukawa, Y. Fujitani, T. Sasaki-Sakamoto, K. Kuroda, S. Nunomura, K. Hayama, T. Terui, C. Ra, Y. Okayama, Expression of Mas-related gene X2 on mast cells is upregulated in the skin of patients with severe chronic urticaria, *J Allergy Clin Immunol* 134 (3) (2014) 622–633. <https://doi.org/10.1016/j.jaci.2014.05.004>.
- [22] J. Meixiong, M. Anderson, N. Limjunyawong, M.F. Sabbagh, E. Hu, M.R. Mack, L. K. Oetjen, F. Wang, B.S. Kim, X.Z. Dong, Activation of mast-cell-expressed Mas-Related G-Protein-coupled Receptors drives non-histaminergic itch, *Immunity* 50 (5) (2019) 1163–1171. <https://doi.org/10.1016/j.immuni.2019.03.013>.
- [23] E. Azimi, V.B. Reddy, E.A. Lerner, Brief communication: MRGPRX2, atopic dermatitis and red man syndrome, *Itch (phila)* 2 (1) (2017) e5.
- [24] V. Cardona, I.J. Ansotegui, M. Ebisawa, Y. El-Gamal, M. Fernandez Rivas, S. Fineman, M. Geller, A. Gonzalez-Estrada, P.A. Greenberger, M. Sanchez Borges, G. Senna, A. Sheikh, L.K. Tanno, B.Y. Thong, P.J. Turner, M. Worm, World allergy organization anaphylaxis guidance 2020, *World Allergy Organ J* 13 (10) (2020) 100472. <https://doi.org/10.1016/j.waojou.2020.100472>.
- [25] X.X. Guo, M.J. Sun, P.Y. Yang, X.C. Meng, R. Liu, Role of mast cells activation in the tumor immune microenvironment and immunotherapy of cancers, *Eur J Pharmacol* 960 (2023) 176103. <https://doi.org/10.1016/j.ejphar.2023.176103>.
- [26] R. Sulisenti, E. Jachetti, Frenemies in the microenvironment: Harnessing mast cells for cancer immunotherapy, *Pharmaceutics* 15 (6) (2023) 1692. <https://doi.org/10.3390/pharmaceutics15061692>.
- [27] R.M. Amini, K. Aaltonen, H. Nevanlinna, R. Carvalho, L. Salonen, P. Heikkilä, C. Blomqvist, Mast cells and eosinophils in invasive breast carcinoma, *BMC Cancer* 7 (2007) 165. <https://doi.org/10.1186/1471-2407-7-165>.
- [28] S. Sakalauskaite, V. Riškevicienė, J. Šengaut, N. Juodžiukynienė, Association of mast cell density, microvascular density and endothelial area with clinicopathological parameters and prognosis in canine mammary gland carcinomas, *Acta Vet Scand* 64 (1) (2022) 14. <https://doi.org/10.1186/s13028-022-00633-2>.
- [29] C. Ueshima, T.R. Kataoka, M. Hirata, A. Furuhashi, E. Suzuki, M. Toi, T. Tsuruyama, Y. Okayama, H. Haga, The killer cell Ig-like receptor 2DL4 expression in human mast cells and its potential role in breast cancer invasion, *Cancer Immunol Res* 3 (8) (2015) 871–880. <https://doi.org/10.1158/2326-6066.CIR-14-0199>.
- [30] M.T. Majorini, V. Cancila, A. Righoni, L. Botti, M. Dugo, T. Triulzi, L. De Cecco, E. Fontanella, E. Jachetti, E. Tagliabue, C. Chiodoni, C. Tripodo, M.P. Colombo, D. Lecis, Infiltrating mast cell-mediated stimulation of estrogen receptor activity in breast cancer cells promotes the luminal phenotype, *Cancer Res* 80 (11) (2020) 2311–2324. <https://doi.org/10.1158/0008-5472.CAN-19-3596>.
- [31] X.S. He, Y. Sui, S. Wang, Application of a stepwise frontal analysis method in cell membrane chromatography, *J Chromatogr B Anal Technol Biomed Life Sci* 1161 (2020) 122436. <https://doi.org/10.1016/j.jchromb.2020.122436>.
- [32] B.S. Suvama, Drug-receptor interactions, *Kathmandu Univ Med J (KUMJ)* 9 (35) (2011) 203–207. <https://doi.org/10.3126/kumj.v9i3.6306>.
- [33] V. Pliska, Thermodynamic parameters of ligand-receptor interactions: computation and error margins, *J Recept Signal Transduct Res* 17 (1–3) (1997) 495–510. <https://doi.org/10.3109/10799899709036623>.
- [34] W.N. Ma, L. Yang, Y.N. Lv, J. Fu, Y.M. Zhang, L.C. He, Determine equilibrium dissociation constant of drug-membrane receptor affinity using the cell membrane chromatography relative standard method, *J Chromatogr A* 1503 (2017) 12–20. <https://doi.org/10.1016/j.chroma.2017.04.053>.
- [35] J. Elst, M. Maurer, V. Sabato, M.A. Faber, C.H. Bridts, C. Mertens, M. Van Houdt, A. L. Van Gasse, M.M. van der Poorten, L.P. De Puyssseleyr, M.M. Hagendorens, V. F. Van Tendeloo, E. Lion, D. Campillo-Davo, D.G. Ebo, Novel insights on MRGPRX2-mediated hypersensitivity to neuromuscular blocking agents and fluoroquinolones, *Front Immunol* 12 (2021) 668962. <https://doi.org/10.3389/fimmu.2021.668962>.
- [36] D. Holowka, M. Wilkes, C. Stefan, B. Baird, Roles for Ca<sup>2+</sup> mobilization and its regulation in mast cell functions: recent progress, *Biochem Soc Trans* 44 (2) (2016) 505–509. <https://doi.org/10.1042/BST20150273>.
- [37] I. Kazama, K. Saito, A. Baba, T. Mori, N. Abe, Y. Endo, H. Toyama, Y. Ejima, M. Matsubara, M. Yamauchi, Clarithromycin dose-dependently stabilizes rat peritoneal mast cells, *Chemotherapy* 61 (6) (2016) 295–303. <https://doi.org/10.1159/000445023>.
- [38] D. Che, T. Zhang, T.X. Zhang, Y. Zheng, Y.J. Hou, S.M. Geng, L.C. He, Clarithromycin-treated chronic spontaneous urticaria with the negative regulation of FcεR1 and MRGPRX2 activation via CD300f, *Int Immunopharmacol* 110 (2022) 109063. <https://doi.org/10.1016/j.intimp.2022.109063>.
- [39] K. Bukowski, M. Kciuk, R. Kontek, Mechanisms of multidrug resistance in cancer chemotherapy, *Int J Mol Sci* 21 (9) (2020) 3233. <https://doi.org/10.3390/ijms21093233>.
- [40] B.A. Baldo, N.H. Pham, Adverse reactions to targeted and non-targeted chemotherapeutic drugs with emphasis on hypersensitivity responses and the invasive metastatic switch, *Cancer Metastasis Rev* 32 (3–4) (2013) 723–761. <https://doi.org/10.1007/s10555-013-9447-3>.
- [41] M. Pagani, S. Bavbek, E. Alvarez-Cuesta, A. Berna Dursun, P. Bonadonna, M. Castells, J. Cernadas, A. Chiriac, H. Sahar, R. Madrigal-Burgaleta, S. Sanchez Sanchez, Hypersensitivity reactions to chemotherapy: an EAACI position paper, *Allergy* 77 (2) (2022) 388–403. <https://doi.org/10.1111/all.15113>.
- [42] M. Pagani, The complex clinical picture of presumably allergic side effects to cytostatic drugs: symptoms, pathomechanism, reexposure, and desensitization, *Med Clin North Am* 94 (4) (2010) 835–852. <https://doi.org/10.1016/j.mcna.2010.03.002>.
- [43] S.M.T. Nguyen, C.P. Rupprecht, A. Haque, D. Pattanaik, J. Yusin, G. Krishnaswamy, Mechanisms governing anaphylaxis: Inflammatory cells, mediators, endothelial gap junctions and beyond, *Int J Mol Sci* 22 (15) (2021) 7785. <https://doi.org/10.3390/ijms22157785>.
- [44] G.R. Gandhi, T. Mohana, K. Athesh, V.E. Hillary, A.B.S. Vasconcelos, M.N. Farias de Franca, M.M. Montalvão, S.A. Ceasar, G. Jothi, G. Sridharan, R.Q. Gurgel, B. Xu, Anti-inflammatory natural products modulate interleukins and related signaling markers in inflammatory bowel disease: A systematic review, *J Pharm Anal* 13 (12) (2023) 1408–1428. <https://doi.org/10.1016/j.jpha.2023.09.012>.
- [45] H.H. Wu, M.Q. Zeng, E.Y.P. Cho, W.Q. Jiang, O. Sha, The origin, expression, function and future research focus of a G protein-coupled receptor, mas-related gene X2 (MrgX2), *Prog Histochem Cytochem* 50 (1) (2015) 11–17. <https://doi.org/10.1016/j.proghi.2015.06.001>.
- [46] M. Yoshioka, N. Fukuiishi, Y. Kubo, H. Yamanobe, K. Ohsaki, Y. Kawasoe, M. Murata, A. Ishizumi, Y. Nishii, N. Matsui, M. Akagi, Human cathelicidin CAP18/LL-37 changes mast cell function toward innate immunity, *Biol Pharm Bull* 31 (2) (2008) 212–216. <https://doi.org/10.1248/bpb.31.212>.
- [47] M. Kulka, C.H. Sheen, B.P. Tancoway, L.C. Grammer, R.P. Schleimer, Neuropeptides activate human mast cell degranulation and chemokine production, *Immunol* 123 (3) (2008) 398–410. <https://doi.org/10.1111/j.1365-2567.2007.02705.x>.
- [48] S. Suvas, Role of substance P neuropeptide in inflammation, wound healing, and tissue homeostasis, *J Immunol* 199 (5) (2017) 1543–1552. <https://doi.org/10.4049/jimmunol.1601751>.
- [49] H. Javid, F. Mohammadi, E. Zahiri, S.I. Hashemy, The emerging role of substance P/neurokinin-1 receptor signaling pathways in growth and development of tumor cells, *J Physiol Biochem* 75 (4) (2019) 415–421. <https://doi.org/10.1007/s13105-019-00697-1>.
- [50] M. Muñoz, R. Covenas, Involvement of substance P and the NK-1 receptor in cancer progression, *Peptides* 48 (2013) 1–9. <https://doi.org/10.3748/wjg.v20.i9.2321>.
- [51] E. Harford-Wright, K.M. Lewis, R. Vink, M.N. Ghabriel, Evaluating the role of substance P in the growth of brain tumors, *Neuroscience* 261 (2014) 85–94. <https://doi.org/10.1016/j.neuroscience.2013.12.027>.
- [52] A. González-Ortega, E. Sánchez-Vaderrábanos, S. Ramiro-Fuentes, M.V. Salinas-Martín, A. Carranza, R. Covenas, M. Muñoz, Uveal melanoma expresses NK-1 receptors and cyclosporin A induces apoptosis in human melanoma cell lines overexpressing the NK-1 receptor, *Peptides* 55 (2014) 1–12. <https://doi.org/10.1016/j.peptides.2014.01.030>.
- [53] D. Singh, D.D. Joshi, M. Hameed, J. Qian, P. Gascón, P.B. Maloof, A. Mosenenthal, P. Rameshwar, Increased expression of preprotachykinin-1 and neurokinin receptors in human breast cancer cells: implications for bone marrow metastasis, *Proc Natl Acad Sci U S A* 97 (1) (2000) 388–393. <https://doi.org/10.1073/pnas.97.1.388>.
- [54] M. Davoodian, N. Boroumand, M. Mehrabi Bahar, A.H. Jafarian, M. Asadi, S.I. Hashemy, Evaluation of serum level of substance P and tissue distribution of NK-1

- receptor in breast cancer, *Mol Biol Rep* 46 (1) (2019) 1285–1293. <https://doi.org/10.1007/s11033-019-04599-9>.
- [55] J.D. Heilborn, M.F. Nilsson, C.I. Jimenez, B. Sandstedt, N. Borregaard, E. Tham, O. E. Sørensen, G. Weber, M. Stähle, Antimicrobial protein hCAP18/LL-37 is highly expressed in breast cancer and is a putative growth factor for epithelial cells, *Int J Cancer* 114 (5) (2005) 713–719, <https://doi.org/10.1002/ijc.20795>.
- [56] X. Chen, X.Q. Zou, G.Y. Qi, Y. Tang, Y. Guo, J. Si, L.H. Liang, Roles and mechanisms of human cathelicidin LL-37 in cancer, *Cell Physiol Biochem* 47 (3) (2018) 1060–1073, <https://doi.org/10.1159/000490183>.